PB 161632

NBS

Technical Note 131

PHOTOIONIZATION OF ATOMS AND MOLECULES

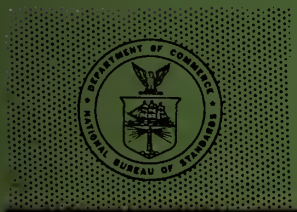

U. S. DEPARTMENT OF COMMERCE
NATIONAL BUREAU OF STANDARDS

THE NATIONAL BUREAU OF STANDARDS

Functions and Activities

The functions of the National Bureau of Standards are set forth in the Act of Congress, March 3, 1901, as amended by Congress in Public Law 619, 1950. These include the development and maintenance of the national standards of measurement and the provision of means and methods for making measurements consistent with these standards; the determination of physical constants and properties of materials; the development of methods and instruments for testing materials, devices, and structures; advisory services to government agencies on scientific and technical problems; invention and development of devices to serve special needs of the Government; and the development of standard practices, codes, and specifications. The work includes basic and applied research, development, engineering, instrumentation, testing, evaluation, calibration services, and various consultation and information services. Research projects are also performed for other government agencies when the work relates to and supplements the basic program of the Bureau or when the Bureau's unique competence is required. The scope of activities is suggested by the listing of divisions and sections on the inside of the back cover.

Publications

The results of the Bureau's research are published either in the Bureau's own series of publications or in the journals of professional and scientific societies. The Bureau itself publishes three periodicals available from the Government Printing Office: The Journal of Research, published in four separate sections, presents complete scientific and technical papers; the Technical News Bulletin presents summary and preliminary reports on work in progress; and Basic Radio Propagation Predictions provides data for determining the best frequencies to use for radio communications throughout the world. There are also five series of nonperiodical publications: Monographs, Applied Mathematics Series, Handbooks, Miscellaneous Publications, and Technical Notes.

A complete listing of the Bureau's publications can be found in National Bureau of Standards Circular 460, Publications of the National Bureau of Standards, 1901 to June 1947 ($1.25), and the Supplement to National Bureau of Standards Circular 460, July 1947 to June 1957 ($1.50), and Miscellaneous Publication 240, July 1957 to June 1960 (Includes Titles of Papers Published in Outside Journals 1950 to 1959) ($2.25); available from the Superintendent of Documents, Government Printing Office, Washington 25, D. C.

NATIONAL BUREAU OF STANDARDS

Technical Note

131

JANUARY 1962

PHOTOIONIZATION OF ATOMS AND MOLECULES

Fred L. Mohler

DISTRIBUTED BY

UNITED STATES DEPARTMENT OF COMMERCE

OFFICE OF TECHNICAL SERVICES

WASHINGTON 25, D. C.

Price $1.25

TABLE OF CONTENTS

Photoionization of Atoms and Molecules

by Fred L. Mohler*

This is a review of experimental results on photoionization of atoms and some molecules. There are some quantitative data on all the alkalies, magnesium, calcium and thallium and all rare gases except xenon. Results are given for the common gases; hydrogen, nitrogen, oxygen, CO, CO_2, NO, N_2O, NO_2, H_2O and CH_4. Autoionization, excitation to a state above the ionization threshold followed by transition to the ionized state, can be an important factor. Often the broad autoionization lines mask the true continuum. There are some mass spectrometric measurements of photoionization products for most of these molecules.

1. INTRODUCTION

The purpose of this report is to give a survey and bibliography of experimental measurements of photoionization and of the continuous absorption bands resulting in photoionization. The scope of this report will include atoms and some simple diatomic and polyatomic molecules. A survey of this subject through 1955 is given in a Handbuch der Physik article by G. L. Weissler [1].

Ever since the publication of Bohr's theory of atomic structure it has been recognized that beyond each absorption series there will be a continuous absorption band arising from removal of an electron from the atom with kinetic energy. Characteristic X-ray absorption spectra are photoionization continua that have been quite systematically studied [2]. The absorption for each X-ray level begins abruptly at the series limit and decreases roughly as the cube of the wavelength λ. A general formula for this absorption is

$$\sigma_n = C_n Z^a \lambda^b$$

where σ_n is the atomic absorption coefficient for each X-ray level K, L_1, L_2, L_3, M_1, M_2, etc., and C_n is a constant involving the quantum numbers of each X-ray level and the threshold wavelength of the level and Z is the atomic number. a is roughly 4 and b ranges from 2.5 to 3.

*Consultant to the Atomic Physics Division, NBS.

In contrast to the X-ray range, the experimental data on photoionization of valence electrons remain to this day quite fragmentary and incomplete. The photoionization bands fall in general in the vacuum ultraviolet which involves serious experimental difficulties. Furthermore, there are relatively few elements that are monatomic in the gas phase. The rare gases are the only elements that are purely monatomic. Vapors of the electro-positive metals are predominantly monatomic, but in most cases diatomic molecules of relatively low stability have also been observed in the vapor [3].

The photoionization absorption is conveniently expressed in terms of the absorption per atom (the effective atomic collision area for the photon) here written as σ. it is also expressed as the absorption per cm, α, in gas at normal pressure and temperature,

$$\sigma = \alpha \times 3.72 \times 10^{-20}.$$

One can measure the absorption of a column of gas at a known pressure, or alternatively one can measure the ion current produced by a measured radiation flux [5,6] in gas at a known pressure. This alternative method can be used in metal vapors at pressures too low to give measurable absorption.

in most atoms there are excited states of the neutral atom which fall above the first ionization threshold, and these states can pass spontaneously,into the ionized state. Excitation of these states gives absorption lines which are commonly unsymmetrically broadened on the short wavelength side and the widths indicate half lives ranging down to 10^{-15} sec or less. These lines have not been observed in emission and presumably radiation transitions are negligible compared with autoionization [4]. Autoionization in some cases makes contributions to the total photoionization that are large compared with the continuous absorption. In the extreme ultraviolet, line emission sources are commonly used and line sources cannot give quantitative information on line absorption processes, although fortuitously the line spectra often overlap the broad absorption lines.

There are some instances of photoionization produced in a two step process by line absorption below the first ionization potential. Thus Foote and Mohler [7] found that there is some ionization by line absorption in cesium vapor. The efficiency of ionization is proportional to the pressure, and it can be explained by the assumption that highly excited atoms react with neutral atoms to form molecule ions [8]. This and other similar pressure dependent reactions will not be included in this survey.

In the photoionization of molecules the number of ions produced may be less than the number of quanta absorbed and the ratio (here expressed in percent) is called the efficiency of photoionization. Commonly the efficiency is low near the threshold.

In the ionization of molecules the products can be either molecule ions or fragment ions, and it requires a mass spectrometric analysis to obtain a complete interpretation of the results. In practice it is best to measure the ionization cross section in a simple ionization chamber and use the mass spectrometric measurement to evaluate relative abundances of different ions.

.2. EXPERIMENTAL METHODS

The rare gases are purely monatomic and a direct measurement of the continuous absorption affords the simplest method of evaluating the atomic cross section for photoionization. There is the complication that the continuous spectra fall in the extreme ultraviolet and nearly all window materials are opaque to this radiation. Effective sources for the far ultraviolet are intense discharges in hydrogen, helium or argon, or high vacuum sparks between metal electrodes. In any case, it is essential to separate the discharge region and the gas being studied. Weissler and his colleagues [1] have used a differential pumping chamber between the source and the spectrometer entrance slit. Ditchburn [36] has found it feasible to use thin sheets of collodion over the slit to separate the discharge and the gas being studied.

High temperatures and chemical reaction with windows are a difficulty in measurements with most of the metal vapors. Ditchburn and his associates [16] have used a tube of the following design to keep windows cool and clear. The metal vapor is confined by two metal plugs to the central half of a nickel tube about 2 meters long. These plugs are about 10 cm long with holes 6 mm in diameter along the axis. The mid-section is held at a temperature which gives a convenient vapor pressure, the plugs are at a slightly higher temperature, and the rest of the tube is cool. Helium at roughly 1 cm pressure is in the tube, and this slows up the diffusion of the metal and keeps it from reaching the windows. The experimental uncertainty in the vapor pressure, temperature data is probably the major source of uncertainty.

Intensity measurements can be made either by a photomultiplier or by photographic densitometry. Electrical measurements can give better precision, but photographs give optimum resolving power which is important when autoionization peaks are present. In measurements at wavelengths of less than 1000A, sources giving line emission spectra are commonly used and autionization cannot be measured quantitatively.

Measurements of photoionization cross sections can be made by passing a beam of radiation through a simple parallel plate ionization chamber in gas at a measured pressure. The beam strikes a thermopile or the sensitized surface of a photomultiplier bulb which measures the photon flux [5]. A surface of sodium salicylate gives a nearly constant quantum sensitivity in the range (to about 1000A) in which it is feasible to calibrate it with a thermopile. Weissler's group have used two or three ionization chambers spaced along a tube containing the gas to measure both the absorption and the photoionization [6].

In pioneer studies of photoionization of cesium vapor, Foote and Mohler [7] used the space charge effect of positive ions on thermionic emission from a hairpin cathode to detect photoionization. When the voltage in a diode is reduced to one or two volts the current is limited by space charge and there is a potential minimum in the region around the filament. If positive ions are produced in this region, they are trapped and neutralize the space charge. One ion can liberate more than 10^4 electrons and this large amplification factor made it simple to measure photoionization as a function of wavelength. Absolute measurements were made at a few wavelengths with a simple ionization chamber and measured radiation flux [19].

Mass spectrometric research on photoionization of molecules is with one notable exception a relatively new field of research. In 1932 Terenin and Popov [9] found that thallium iodide, bromide and chloride are ionized by radiation transmitted by a quartz monochromator. A simple magnetic spectrometer showed that the ions are Tl^+ and I^- or Br^- for the iodide or bromide. The ion current reached a peak value near 2125A for Tl I and 2000A for Tl Br. The cross section for photoionization was of the order of 10^{-17} cm^2.

In recent years Hurzeler, Inghram, and Morrison [10] have used a mass spectrometer to study ionization products produced by resolved ultraviolet radiation transmitted by a lithium fluoride window. They reported on a variety of organic molecules which are ionized by radiation of wavelength greater than 1080A. Weissler, Samson, Ogawa and Cook [46] measured mass spectra of photoionization products without a window between the monochromator and the ionization chamber, and preliminary results have been published for O_2, N_2, CO, NO, CO_2, N_2O and NO_2.

Lassettre and his staff at Ohio State University have made careful measurements of the probability of inelastic scattering of 500 ev electrons as a function of the energy lost in collision. Studies include helium, nitrogen, oxygen, carbon monoxide, carbon dioxide and water [13]. He assumes with supporting evidence that at 500 ev the Born approximation is valid and probabilities of inelastic collision can be related to probabilities of photon absorption. This affords an alternative method of deriving photoionization cross sections that avoids the difficulties of far ultraviolet research. Results seem to be consistent with optical measurements, but resolving power is less and except in helium transitions to discrete states tend to mask the continua.

3. EXPERIMENTAL RESULTS

3.1. Foreword

The following summary of experimental results gives photoionization cross sections for atoms and some molecules. The section on molecules is limited to common diatomic molecules and simple polyatomic molecules, with particular attention to molecules that might be found in the upper air. With a few exceptions, the list is limited to researches affording a quantitative basis for estimating atomic or molecular cross sections for photoionization.

For each atom, following the chemical symbol for the element, the ionization threshold is given in angstrom units and in electron volts. The configuration is given for the normal state or for the ionized states in customary spectral notation. Data are taken from Charlotte Moore's "Circular on Atomic Energy Levels" [11]. The elements are arranged according to columns of the periodic table beginning with hydrogen and the alkalies.

For molecules spectral notation of the normal state is not given. The threshold is commonly the first of a group of "Rydberg series limits" and some information on the other limits is given.

Figures showing atomic or molecular cross sections as a function of wavelength or electron volts are given for nearly all the atoms and molecules. These are all taken from the sources indicated without editing and a variety of coordinates are used. In this field a common unit of cross section is the "megabarn", Mb, which is 10^{-18} cm^2.

3.2. Photoionization Cross Sections of Atoms

H λ_o = 912A 13.595 ev Normal state $1s\ ^2S_{1/2}$

There are no experimental measurements of σ, but the theory is reliable and gives as a good approximation [14]

$$\sigma = 6.33 \times 10^{-18} (\lambda/\lambda_o)^3$$

Li λ_o = 2300A 5.390 ev Normal state $2s\ ^2S_{1/2}$.

Tunstead [15] measured the absorption cross section in the range 2300A to 1800A. σ_o (2300A) is $2.5 \pm .5 \times 10^{-18}$ cm^2. σ decreases with decreasing wavelength, and σ (1800A) is 1.35×10^{-18}. It decreases in this range as $\lambda^{2.5}$. See figure 1.

Na λ_o = 2412A 5.138 ev Normal state $3s\ ^2S_{1/2}$

Ditchburn, et al., [16] measured the absorption cross section in the range 2412 to 1600A, and Hudson [17] has extended the measurements to 1100A.

σ_o (2412A) = $.116 \pm .012 \times 10^{-18}$ cm^2 and drops sharply to $.013 \times 10^{-18}$ at 1950A and rises to a sharp maximum $\sigma = .4 \times 10^{-18}$ at 1400A, and is less than $.01 \times 10^{-18}$ at 1100A. See figure 2. A correction for molecular absorption has been made [16] by measuring absorption as a function of pressure and extrapolating to low pressure.

K λ_o = 2856A 4.339 ev Normal state $4s\ ^2S_{1/2}$

Ditchburn, Tunstead and Yates [18] measured the absorption coefficient to 1600A and measurements at different pressures gave a correction for some molecular absorption.

σ_o (2856A) = $.012 \pm .003 \times 10^{-18}$ cm^2 and drops to $.008 \times 10^{-18}$ at 2700A, and rises to $.24 \times 10^{-18}$ at 1600A. See figure 3.

Photoionization measurements confirm the shape of the absorption curve to 2200A [19,20].

K_2 amounts to less than 3 percent of the vapor at the highest vapor pressures and the absorption is negligible to 2100A but σ (K_2) rises to roughly 10×10^{-18} at 1700A [22].

Rb λ_o = 2968A 4.176 ev Normal state $5s\ ^2S_{1/2}$

Mohler and Boeckner [19] measured photoionization in the range 2968A to 2300A. They used the space charge effect combined with a measurement in a simple ionization chamber with radiation of measured quantum flux.

σ_o (2968A) = 0.11 x 10^{-18} cm^2. σ drops rapidly with decreasing λ reaching nearly 0 at 2550A and remains low to 2300A. See figure 4.

Beutler [21] has observed 39 absorption lines in the range 810A to 594A which presumably give autoionization. They fall in series that converge to ^3P and ^1P limits of the configuration $4p^5$ 5s.

Cs λ_o = 3184A 3.893 ev Normal state $6s\ ^2S_{1/2}$

Braddick and Ditchburn [22] measured the absorption from 3184A to 2300A.

σ_o (3184A) = .22 ± .01 x 10^{-18} cm^2 and drops to .078 x 10^{-18} near 2800A and rises to .15 x 10^{-18} near 2400A. See figure 5. The absorption is proportional to the pressure. Mohler and Boeckner [19] measured the photoionization in this range. Their values are σ_o = .23 ± .02 x 10^{-18}. σ reaches a minimum of .043 x 10^{-18} near 2600A and rises to .08 x 10^{-18} near 2200A. Beutler and Guggenheimer [23] find absorption lines beginning at 999A which converg to ^3P and ^1P limits 721A, 719A, 651A and 649A of the configuration $5p^5$ 6s.

Mg λ_o = 1610A 7.64 ev Ionized state $3s\ ^2S$

Ditchburn and Marr [24] have measured absorption from 1610A to 1450A. σ_o (1610A) is 1.18 ± .25 x 10^{-18} cm^2 and σ decreases sharply to 0.2 x 10^{-18} at 1450A. The absorption is directly proportional to the pressure. See figure 6.

Ca λ_o = 2028A 6.11 ev Ionized state $4s\ ^2S$

λ_o = 1589A 7.82 ev Ionized state $3d\ ^2D_{5/2\ 3/2}$

Jutsum [26] and Ditchburn and Hudson [25] have measured absorption in the range 2028A to 1100A. This is characterized by continuous absorption beyond 2028A and 1589A and by two series of absorption lines, much broadened by autoionization in the range 1900A to 1589A. The absorption series involve double excitation of the two valence electrons into a 3d level and into p levels. For the continuum σ_o (2028A) = .45 ± .07 x 10^{-18} cm^2 and this drops sharply to zero near 1950. In the range 1900A to 1589A it rises to about 0.45 x 10^{-18} but this range is partly masked by line absorption. At 1589A it rises to 0.9 x 10^{-18} and falls to a flat minimum of .32 x 10^{-18} near 1250A and is .55 x 10^{-18} at 1100A.

The first autoionization lines of the singlet P series have peak absorption coefficients of 30×10^{-18} and 70×10^{-18} and half-widths of 615 cm^{-1} and 69 cm^{-1}. See figures 7 and 8.

In λ_o = 2143A 5.785 ev Normal state $5s^2\ 5p\ ^2P_{1/2}$

Garton [29] has published a qualitative description of the absorption from 2143A to 1400A. Absorption decreases from 2143A to nearly zero at 1800A and five intense diffuse absorption lines at 1757.3A, 1740.9A, 1711.1A, 1676.2A and 1648.7A dominate in intensity. These lines come from the configuration $5s\ 5p^2$. Marr [30] has measured the maximum atomic absorption coefficient of the 1757A line as about 10^{-16} cm^2 and estimates the continuous absorption coefficient σ_o (2143A) to be one percent or less of this or of the order of 10^{-18}.

Tl λ_o = 2030A 6.106 ev Normal state $6s^2\ 6p\ ^2P_{1/2}$

Marr [27] has measured the absorption in the range 2030A to 1450A. Very intense wide autoionization lines tend to mask the continuum [28]. σ_o (2030A) = 4.5×10^{-18} cm^2. σ drops to 2.1×10^{-18} at 2010A. At 1950A it is 4.8×10^{-18} and drops to 0.7×10^{-18} at 1750A. Three autoionization peaks are

λ	σ max.	f number	half width	half life	Term
2007	12×10^{-18}	.005	300 cm^{-1}	$18 \pm 5 \times 10^{-15}$ sec	$^4P_{3/2}$
1610	150×10^{-18}	$.52 \pm .09$	2450 cm^{-1}	2.2×10^{-15} sec	^2D
1490	30×10^{-18}	.005	———	———	^2P

These come from the configuration $6s\ 6p^2$. The "f number" for the continuum is 0.025. See figure 9.

He λ_o = 504.3A 24.58 ev Ionized state $1s\ ^2S$

Lee and Weissler [31] measured the absorption in the range 504A to 240A. Axelrod and Givens [32] extended the measurements to 150A. Dershem and Schein [33] in 1931 measured the absorption coefficient of K α of carbon (λ = 44.6A) in He.

Lee and Weissler [31] find σ_o at 504A = $7.1 \pm .7 \times 10^{-18}$ cm^2. σ (400A) = 4.0×10^{-18}, σ (300A) = 1.66×10^{-18}, σ (240A) = $.92 \times 10^{-18}$. Axelrod and Givens [32] find somewhat larger values at the shorter wavelengths. σ (300A) = 2.3×10^{-18}, σ (250A) = 1.6×10^{-18}, σ (200A) = $.95 \times 10^{-18}$, σ (170A) = $.73 \times 10^{-18}$ cm^2. See figure 10. Dershem and Schein [33] find σ (44.6A) = 0.0238×10^{-18} cm^2.

Between 504A and 200A, σ decreases as $\lambda^{2.18}$. Between 200A and 44.6A, σ decreases as $\lambda^{2.46}$.

Wheeler [34] has computed the theoretical value as $\sigma_o = 7.4 \times 10^{-18}$.

Ne	λ_o = 576.7A	21.56 ev	Ionized state	$2s^2\ 2p^5\ {}^2P_{3/2}$
	574.9A		Ionized state	$^2P_{1/2}$
	256A	48.5 ev	Ionized state	$2s\ 2p^6\ {}^2S$

Lee and Weissler [35] and Ditchburn [36] have measured the absorption to 240A and 200A respectively. Data are consistent within the range of experimental uncertainty. Ditchburn gives σ_o (577A) = 4×10^{-18} cm^2 and σ rises to a flat maximum of 8×10^{-18} near 400A and falls to 5×10^{-18} near 256A and jumps to 7.5×10^{-18} at 256A and falls to 5×10^{-18} near 200A. See figure 11.

Dershem and Schein [33] find for the absorption coefficient of carbon K α (44.6A) $\sigma = 0.436 \times 10^{-18}$ cm^2. From 256A to 44.6A σ decreases as $\lambda^{1.6}$.

Ar	λ_o = 786.7A	15.75 ev	Ionized state	$3s^2\ 3p^5\ {}^2P_{3/2}$
	777.96A	15.91 ev	Ionized state	$^2P_{1/2}$
	424A	29.3 ev	Ionized state	$3s\ 3p^6\ {}^2S$

Po Lee and Weissler [35] measured the absorption in the range 787A to 360A. There is autoionization by absorption lines between 786.7A and 778A [37]. There are also autoionization peaks in the range 535A to 428A, but measurements are not quantitative as a line emission source was used in this range.

The continuous absorption measurements give σ_o (778A) = 36×10^{-18} cm^2. This is nearly constant to 700A and drops smoothly to 14×10^{-18} near 424A. It jumps to 19×10^{-18} at 424A and falls smoothly to 8×10^{-18} at 360A. See figure 12.

Wainfan, Walker and Weissler [38] measured photoionization in the range 787A to 500A with values consistent with the absorption measurements.

Kr	λ_o = 885A	13.996 ev	Ionized state	$4s^2\ 4p^5\ {}^2P_{3/2}$
	845A	14.66 ev	Ionized state	$^2P_{1/2}$
	326A	38.5 ev	Ionized state	$4s\ 4p^6\ {}^2S$

Anne Pery-Thorne and Garton [39] have measured absorption in the range 885A to 500A. The continuum was measured by photomultiplier and the line absorption by photographic densitometry.

Between 885A and 845A the continuum is partially masked by broad lines [40] converging at $^2P_{1/2}$.

σ_o (885A) is about 30 x 10^{-18} cm^2 and σ_o (845A) is 37 ± 7 x 10^{-18}. σ remains nearly constant to 600A and drops to 30 x 10^{-18} at 500A. See figure 13. They measured the integral of the absorption across each line for doublets between 881A and 851A. The f numbers for the first two doublets are: 881A, f = 0.0431; 869.5A, f = 0.0235; 862.7A, f = 0.0143; 858.5A, f = 0.0086.

3.3. Photoionization Cross Section of Some Molecules

H_2 λ_o = 804.13A [43] 15.42 ev

Lee and Weissler [41] measured the continuous absorption in the range 800A to 300A, and found autoionization bands superposed on the continuum in the range 770A to 670A. Beutler and Junger [43] have described the band system giving rise to autoionization. The rotational fine structure of this band system suddenly become diffuse beyond 804.13A.

The continuum rises abruptly from 804A to a value of σ = 7.4 x 10^{-18} cm^2 near 750A, and drops gradually to 4 x 10^{-18} at 400A and less than .7 x 10^{-18} at 300A. See figure 14.

Wainfan, Walker and Weissler [38] measured photoionization cross section and photoionization efficiency from 800A to 650A. The efficiency is nearly 100 percent and the maximum value of σ_i = 8.3 x 10^{-18} cm^2. Values for the bands are not quantitative, as a line source was used.

Schönheit [42] has published a note on the mass spectrum of the photoionization products. At 637A (19.5 ev) the relative abundance of ions was: H_2^+ is 1.00; H^+ is 0.10; H_3^+ (from collisions of H_2^+ and H_2) is 0.03. The appearance potential of H^+ is 18.05 ev [48].

N_2 λ_o = 795.74A 15.503 ev [47]

λ_o belongs to a group of Rydberg series limits at 796A, 742A, 661A and 526A. Band systems converging at levels beyond 796A, give autoionization peaks superposed on the conbinuum [47]. Measurements of autoionization are not quantitative.

Weissler, Po Lee and Mohr [44] measured absorption in the range 796A to 300A, and Curtis [45] measured absorption to 150A.

Wainfan, Walker and Weissler [38] measured photoionization in the range 796A to 500A and found nearly 100 percent efficiency beyond 750A.

Weissler, Samson, Ogawa and Cook [46] measured the mass spectrum of the ions produced by photoionization for wavelengths down to 400A.

Weissler, et al., [44] find the continuum rises abruptly from the threshold to $\sigma = 25 \times 10^{-18}$ near 750A. σ is about 22×10^{-18} at 670A and 27×10^{-18} near 660A and falls almost linearly to about $.7 \times 10^{-18}$ at 300A. See figure 15. Curtis [45] finds a similar curve but gives absolute values about half the values reported by others. Mass spectra show that N^+ appears at 510A (24.3 ev) and from 480A to 400A the abundance is nearly constant and about one percent of N_2^+. The threshold for N^+ is consistent with appearance potential measurements [48].

O_2 $\lambda_o = 1026.5A$ 12.09 ev

Rydberg series converge to limits 1026.5A, 770A, 729A, 681A and 611A [47]. Autoionization peaks occur in this range.

Weissler and Po Lee [49] and Po Lee [50] have measured absorption in the range 1300A to 200A.

Watanabe and Marmo [51] measured photoionization and absorption in the range 1026A to 850A using a continuous emission source.

Wainfan, Walker and Weissler [38] measured photoionization cross sections to 473A, and Weissler, Samson, Ogawa and Cook [46] measured the mass spectrum.

Po Lee [50] used relatively high resolution. In the range 1026A to 675A autoionization peaks partially mask the true continuum. The continuum rises from the threshold to a value of $\sigma = 2.0 \times 10^{-18}$ cm^2 at 970A, 4.0×10^{-18} at 920A, and 3.0×10^{-18} at 850A. From 850A to 740A it is masked by autoionization bands, but rises to about 20×10^{-18} at 740A and remains about this value to 500A and drops to 12×10^{-18} near 200A. See figure 16.

Watanabe and Marmo [51] measured the efficiency of ionization from 1026A to 850A. It ranges from 50 percent to 100 percent, and the more intense autoionization bands are about 5 times as strong as the background continuum. Values of σ for the continuum are consistent with Po Lee's values. Photoionization measurements in the far ultraviolet [38] give a nearly constant value of $\sigma_i = 25 \times 10^{-18}$ cm^2 in the range 700A to 473A. This is in fair agreement with Po Lee's absorption measurements ($\sigma = 20 \times 10^{-18}$).

The mass spectrum [46] shows that O^+ appears at 662A (18.8 ev) and rises to a peak near 630A. A second nearly equal peak begins at 603A (20.7 ev). There is some evidence of a third increase near 530A, (23.4 ev). The three critical potentials could give the products O^+ (^4S) + O (^3P), O^+ (^4S) + O (^1D) and O^+ (^4S) + O (^1S) at 18.7 ev, 20.7 ev and 22.9 ev. O^+ currents are roughly 10 percent of the O_2^+ currents and make a relatively small contribution to the total absorption. The O_2^+ curve gives a series of six sharp peaks, probably from autoionization, that conceal the continuum found by Po Lee using higher resolving power.

CO λ_o = 884.7A 13.94 ev [53]

Three Rydberg series limits are at 884.7A, 749.7A, and 630.2A [52, 53].

Sun and Weissler [55] measured the absorption in the range 885A to 374A.

Watanabe [54] measured the photoionization near the threshold.

Weissler, Samson, Ogawa and Cook [46] measured photoionization with a mass spectrometer to 400A.

Photoionization begins with a steep increase at the threshold 884.7A. The continuum, partially masked by autoionization peaks, has a broad flat maximum near 500A of $\sigma = 18 \times 10^{-18}$ cm^2. It is 15×10^{-18} or more from 700A to 400A, and 13×10^{-18} cm^2 at 374A. See figure 17.

C^+ appears near 596A (20.8 ev). It remains less than one percent of CO^+ to 556A (22.3 ev) and then increases to two percent of CO^+. There is some evidence of increases at 24.8 ev and 26.4 ev. These critical potentials have also been observed in electron impact studies [48] and are ascribed to transitions to C^+ (^2P) + O^- (^2P), C^+ (^2P) + O (^3P), C^+ (^2P) + O (^1D) and C^+ (^2P) + O (^1S). O^+ was not observed in photoionization, but is produced by electron impact ionization at 24.7 ev [48].

CO_2 λ_o = 900A 13.79 ev [56]

There is a second Rydberg series limit at 690A, 18.07 ev [56].

Sun and Weissler [55] measured the absorption coefficient in the range 900A to 374A. Nicole Damany-Astoin, et al., [57] measured absorption to 167A.

Wainfan, Walker, and Weissler [38] measured photoionization cross sections and efficiencies to 473A.

Weissler, Samson, Ogawa and Cook [46] measured photoionization in a mass spectrometer to 450A.

The photoionization continuum rises sharply from the threshold to $\sigma = 19 \times 10^{-18}$ cm^2 near 800A and near 690A rises again reaching a flat maximum near 600A of 32×10^{-18} cm^2 (Sun and Weissler [55]) or 29×10^{-18} (Damanay-Astoin [57]). See figure 18. Damanay-Astoin finds a minimum at 415A (29.6 ev) with $\sigma = 16 \times 10^{-18}$ cm^2 [57], and σ rises sharply to a broad maximum of 24×10^{-18} cm^2 near 370A. There is a second sharp minimum of $\sigma = 9 \times 10^{-18}$ cm^2 at 294A (42 ev) and a sharp rise to a third maximum of $\sigma = 23 \times 10^{-18}$ near 270A. From this point σ decreases smoothly to zero at 167A.

Wainfan, et al., find a photoionization efficiency ranging from 60 to 100 percent from 900A to 473A. There are many autoionization peaks in the range covered.

Mass spectra show O^+ increasing to a peak at 646A (19.2 ev) at 610A (20.3 ev) and at 556A (22.3 ev). The cross section at 630A for σ (O^+) is about 1.4×10^{-18}. CO^+ appears near 636A (19.5 ev) and increases at 605A (20.5 ev). The cross section at 630A is σ (CO^+) = $.3 \times 10^{-18}$ cm^2. Appearance potentials of O^+ at 19.2 ev and at 22.3 ev are correlated with processes, $CO + O^+$ (^4S) and O^+ (^2D). The two appearance potentials of CO^+ could be ascribed to $CO^+ + O^-$ (^2P) and $CO^+ + O$ (^3P) but there is some excess kinetic energy [46].

NO $\lambda_o = 1340$A 9.25 ev [58]

There are also Rydberg series limits [58] at 871.5A (14.15 ev), 748.5A (16.48 ev), 678.4A (18.19 ev) and 676.8A (18.23 ev).

Sun and Weissler [60] measured absorption in the range 1800A to 374A, and Granier and Astoin [63] extended the range to 150A.

Watanabe [59] measured photoionization with a continuous source, and good resolution showing separate vibration states of NO and NO^+. See figure 19. Walker and Weissler [61] measured photoionization efficiency to 640A.

Weissler, Samson, Ogawa and Cook [46] measured photoionization in a mass spectrometer.

The photoionization continuum increases almost linearly except for vibration fine structure from 1340A to a value of 18×10^{-18} cm^2 near 900A, drops to about 8×10^{-18} near 780A, rises to a flat maximum of 20×10^{-18} near 600A, drops to 13×10^{-18} at 308A, rises to a maximum of 20×10^{-18} near 260A and falls to 12×10^{-18} near 200A. There are autoionization peaks in most of this spectrum. Figure 20 gives the spectrum to 300A.

O^+ appears near 636A (19.5 ev), reaches a flat maximum near 620A and rises again at 600A (20.7 ev) to a second flat maximum. The O^+ current is at the maximum about 2 percent of the NO^+ current in this range. N^+ appears at 570A (21.8 ev) and rises to a maximum near 540A of about 5 percent of the NO^+ current. O^+ probably comes from the dissociation into O^+ (^4S) + N (^4S) and N (^2D) at 19.5 ev and 20.7 ev respectively. N^+ comes from N^+ (^3P) + O (^3P) [46].

N_2O λ_o = 961A 12.94 ev [62]

Other Rydberg series limits give energy levels of 16.39 ev, 16.55 ev and 20.10 ev [62].

Astoin and Grainier [64] measured the absorption to 160A.

Walker and Weissler [61] measured the photoionization efficiency and cross section in the range 960A to 687A. Weissler, Samson, Ogawa and Cook [46] measured the mass spectrum of the photoionization products.

The photoionization continuum rises sharply from the threshold to a flat maximum near 700A of 32 x 10^{-18} cm^2 [64], or 30 x 10^{-18} cm^2 [61]. There is a minimum of 17 x 10^{-18} cm^2 near 500A, a second flat maximum near 360A of 30 x 10^{-18} cm^2, a well defined minimum at 263A of about 13 x 10^{-18} cm^2, a third maximum of the same size near 300A and the absorption drops to 4 x 10^{-18} at 160A. There are many autoionization peaks in the entire range. See figure 21. NO^+ begins near 810A (15.3 ev) and rises rather irregularly to a value at 650A of 1.3 times the N_2O^+ current and remains about 30 percent greater than N_2O^+ to 500A. N_2^+ appears near 710A (17.4 ev) and rises abruptly to a value about 16 percent of N_2O^+ and remains of this magnitude to 500A. N^+ appears at 620A (20.0 ev) and is roughly 10 percent of N_2O^+. O^+ appears near 810A, 15.3 ev and is roughly 10 percent of N_2O^+. See figure 22.

NO_2 λ_o = 1270A 9.78 ev [65]

Nakayama, Kitamura and Watanabe [65] measured the photoionization from the threshold to 1080A. Weissler, Samson, Ogawa and Cook [46] measured the mass spectrum in the range 1100A to 500A.

Nakayama, et al., find the ionization efficiency very low (.03 to 2 percent) at λ greater than 1200A. There is an increase in the ionization continuum at 1145A (10.83 ev). Near 1100A σ_i is about 2.2 x 10^{-18} cm^2.

Weissler, et al., find both NO_2^+ and NO^+ appearing near 1100A (11.3 ev). Beyond 950A, NO^+ becomes greater than NO_2^+ and at 645A is 3.5 x NO_2^+. Both NO_2^+ and NO^+ curves show 5 or 6 sharp peaks in the range 1100A to 500A. Four of these seem to be common to both curves. They may well be autoionization peaks, but this is an opinion of the reviewer.

O^+ appears at 17.6 ev (700A) and rises to a value of about .75 x NO_2^+ at 645A. Weissler, et al., do not give absolute values of σ for these ionization processes. There is conflicting evidence as to the first ionization potential in electron impact research [48] as well as in these experiments. Nakayama, et al., suggest that 10.83 ev may be the appearance potential for $NO_2 \rightarrow NO^+$ and O^-. Weissler, et al., give this as 11.3 ± .4 ev.

H_2O λ_o = 986A 12.59 ev [66]

Watanabe [66] measured the photoionization threshold. Nicole Astoin [67] measured the continuous absorption coefficient in the range 986A to 160A. There is banded absorption superposed on the continuum. Wainfan, Walker and Weissler [38] measured the photoionization efficiency and cross section in the range 986A to 450A. The efficiency is about 40 percent in the range 986A to 900A, and from 950A to 450A is from 70 to 100 percent. σ_i rises at a fairly constant rate to 20 x 10^{-18} cm^2 near 625A [38]. See figure 23. Nicole Astoin finds for σ_a a value of 21 x 10^{-18} cm^2 at 625A. It drops to a sharp minimum of 11 x 10^{-18} at 512A and rises to 28 x 10^{-18} cm^2 at 435A and falls to 2 x 10^{-18} cm^2 at 167A. The experimental uncertainties are about 20 percent. Mass spectra of the ions have not been studied.

CH_4 λ_o = 955A 12.99 ± .01 ev [66]

Watanabe [66] has measured the photoionization threshold. Sun and Weissler [68] and Ditchburn [69] have measured the continuous absorption to 400A and 300A respectively. Wainfan, Walker and Weissler [38] have measured the efficiency of photoionization and the photoionization cross section to 500A.

The efficiency of ionization increases from 0 to 100 percent between 955A and 800A, σ_i rises sharply to a flat maximum of 39 x 10^{-18} cm^2, 44 x 10^{-18} cm^2 or 60 x 10^{-18} near 800A using measurements of Sun and Weissler [68], Ditchburn [69] or Wainfan, Walker and Weissler [38] respectively, and the ionization efficiency data of the latter. σ_i decreases regularly with decreasing wavelength to 13.1 x 10^{-18} cm^2 at 374A and 4 x 10^{-18} cm^2 at 278A according to Ditchburn (Sun and Weissler give a nearly equal value at 374A). See figure 24.

The mass spectrum of photoionization products has not been studied. The σ_i (λ) curve is simpler than those found for the diatomic and triatomic molecules with no evidence of autoionization states or higher ionization potentials.

4. SUMMARY

It is evident that much more research is needed in the field of photoionization of atoms and simple molecules. Thus, while some work has been done on all the alkali vapors, only in the case of sodium do the measurements extend far enough to permit an estimation of the f number of the continuum. There is some data on all the rare gases except xenon and something on four other elements. In the case of molecules, the reviewer has limited this report to a few common gases. There are data on photoionization thresholds for several hundred polyatomic molecules [67] and in some cases there are measurements of σ from the threshold to about 1000A.

Quantitative measurements of autoionization transitions are a matter of research interest but it requires a continuous spectrum emission source to measure the integral of σ across the line, and such measurements have not been extended into the far ultraviolet. In some atomic spectra and in nearly all molecular spectra the autoionization peaks interfere seriously with measurements of the continuum. Good resolution is necessary to distinguish the continuum from the autoionization peaks and in complicated spectra photographic methods seem to afford the most conclusive data in spite of the inherent limitations of photographic densitometry. However, electrical methods and mass spectrometry are required to interpret the results in the case of molecules.

The magnitudes of the photoionization cross sections and the variation with wavelength show a wide variation. Thus, for atoms, σ near the threshold ranges from $.012 \times 10^{-18}$ for potassium to 36 and 37×10^{-18} for argon and krypton. The figures illustrate the wide variation in the shape of the curves of σ versus wavelength.

5. REFERENCES

[1] Weissler, G. L., Handbuch der Physik 21, 306-341 (Springer, Berlin, 1956).
[2] Bothe, W., Handbuch der Physik, 2nd Ed. 23/2, p. 8 (Springer, Berlin, 1933).
[3] Gaydon, A. G., Dissociation energies and spectra of diatomic molecules, (John Wiley and Sons, New York, (1947).
[4] Beutler, H., Z. Physik 86, 495-515 (1933).
[5] Johnson, F. S., Watanabe, K. and Tousey, R., J. Opt. Soc. Am. 41, 702-8 (1951).
[6] Wainfan, N., Walker, W. C. and Weissler, G. L., J. Appl. Phys. 24, 1318-21 (1953).
[7] Foote, P. D. and Mohler, F. L., Phys. Rev. 26, 195-207 (1925).
[8] Mohler, F. L. and Boeckner, C., J. Research NBS 5, (1930) RP186.
[9] Terenin, A. and Popov, B., Physik Z. Sowjetunion 2, 299-318 (1932).
[10] Hurzeler, H., Inghram, M. G. and Morrison, J. D., J. Chem. Phys. 28, 1, 76-82 (1958).
[11] Moore, Charlotte E., Atomic energy levels, NBS Circular 467, Vol. 1 (1949), Vol. 2 (1952), Vol. 3 (1958).
[12] Watanabe, K., Nakayama, T. and Mott'l, J., Final report on ionization potentials of molecules by a photoionization method, OOR No. 1624 (Dec. 1959).
[13] Lassettre, E. N., et al., Ohio State University Research Foundation Reports to AFCRC, Reports 1 to 12 (1953 to 1958).
[14] Sugiura, Y., Sci. Papers Inst. of Phys. and Chem. Research (Tokyo) 11, 1-80 (1929).
[15] Tunstead, J., Proc. Phys. Soc. (London) A66, p. 304 (1953).
[16] Ditchburn, R. W., Jutsum, P. J. and Marr, G. V., Proc. Roy. Soc. (London) A219, 89-101 (1953).
[17] Hudson, R. D., Am. Phys. Soc. Bul. 2, 5, 495 (1960); A project report to Air Force Research Center (June 28, 1960) unpublished.
[18] Ditchburn, R. W., Tunstead, J. and Yates, J. G., Proc. Roy. Soc. (London) A181, 386-399 (1942-43).
[19] Mohler, F. L. and Boeckner, C., J. Research NBS 3, 303-314 (1929) RP96.
[20] Lawrence, E. O. and Edlefson, N. E., Phys. Rev. 34, 233-242 and 1056-1060 (1929).
[21] Beutler, H., Z. Physik 91, 131-150 (1934).
[22] Braddick, H. J. J. and Ditchburn, R. W., Proc. Roy. Soc. (London) A150, 478-486 (1935).
[23] Beutler, H. and Guggenheimer, K., Z. Physik 88, 25-42 (1934).
[24] Ditchburn, R. W. and Marr, G. V., Proc. Phys. Soc. (London) A66, 655-656 (1953).
[25] Ditchburn, R. W. and Hudson, R. D., Proc. Roy. Soc. (London) A256, 53-61 (1960).
[26] Jutsum, P. J., Proc. Phys. Soc. (London) A67, 190-191 (1954).
[27] Marr, G. V., Proc. Roy. Soc. (London) A224, 83-89 (1954).
[28] Beutler, H. and Demeter, W., Z. Physik 91, 143-150 and 202-217 (1934).
[29] Garton, W. R. S., Nature 166, p. 150 (1950).

[30] Marr, G. V., Proc. Phys. Soc. (London) A67, 196-197 (1954).
[31] Po Lee and Weissler, G. L., Phys. Rev. 99, 540-542 (1955).
[32] Axelrod, N. N. and Givens, M. P., Phys. Rev. 115, p. 97 (1959).
[33] Dershem, E. and Schein, M., Phys. Rev. 37, 1238-1245 (1931).
[34] Wheeler, J. A., Phys. Rev. 43, 258-263 (1933).
[35] Po Lee and Weissler, G. L., Proc. Roy. Soc. (London) A220, 71-76 (1953).
[36] Ditchburn, R. W., Proc. Phys. Soc. (London) 75, 461-462 (1960).
[37] Beutler, H., Z. Physik 93, 177-196 (1935).
[38] Wainfan, N., Walker, W. C. and Weissler, G. L., Phys. Rev. 99, 542-549 (1955).
[39] Pery-Thorne, Anne and Garton, W. R. S., Proc. Phys. Soc. (London) 76, 833-843 (1960).
[40] Beutler, H. and Demeter, W., Z. Physik 91, 218-229 (1934).
[41] Po Lee and Weissler, G. L., Astrophys. J. 115, 570-571 (1952).
[42] Schonheit, E., Z. Naturforsch. 15A, 9, 841-842 (1960).
[43] Beutler, H. and Junger, H. O., Z. Physik 100, 80-94 (1936).
[44] Weissler, G. L., Po Lee and Mohr, E. I., J. Opt. Soc. Am. 42, 84-90 (1952).
[45] Curtis, J. P., Phys. Rev. 94, 908-910 (1954).
[46] Weissler, G. L., Samson, J. A. R., Ogawa, N. and Cook, G. R., J. Opt. Soc. Am. 49, 338-349 (1959).
[47] Tanaka, Y. and Takamine, T., Sci. Papers Inst. Phys. Chem. Research (Tokyo) 39, 427-436 and 437-446 (1941-42).
[48] Field, F. H. and Franklin, J. L., Electron impact phenomena (Academic Press, New York, 1957).
[49] Weissler, G. L. and Po Lee, J. Opt. Soc. Am. 42, 200-203 (1952).
[50] Po Lee, J. Opt. Soc. Am. 45, 703-709 (1955).
[51] Watanabe, K. and Marmo, F. F., J. Chem. Phys. 25, 5, 965-971 (1956).
[52] Tanaka, Y., Sci. Papers Inst. Phys. Chem. Research (Tokyo) 39, 467-474 (1941-42).
[53] Takamine, T., Tanaka, Y. and Iwata, M., Sci. Papers Inst. Phys. Chem. Research (Tokyo) 40, 371-378 (1942-43).
[54] Watanabe, K., J. Chem. Phys. 26, 3, 542-547 (1957).
[55] Sun, H. and Weissler, G. L., J. Chem. Phys. 23, 9, 1625-1628 (1955).
[56] Tanaka, Y., Jursa, A. S. and LeBlanc, F. J., J. Chem. Phys. 32, 4, 1199-1205 (1960).
[57] Damanay-Astoin, N., Sanson, L. and Bonnelle, M. C., Compt. Rend. 250, 10, 1824-1826 (1960).
[58] Tanaka, Y., Sci. Papers Inst. Phys. Chem. Research (Tokyo) 39, 456-466 (1941-42).
[59] Watanabe, K., J. Chem. Phys. 22, 9, 1564-1570 (1954).
[60] Sun, H. and Weissler, G. L., J. Chem. Phys. 23, 1372-1373 (1952).
[61] Walker, W. C. and Weissler, G. L., J. Chem. Phys. 23, p. 1962 (1955).
[62] Tanaka, Y., Jursa, A. S. and LeBlanc, F. J., J. Chem. Phys. 28, 350-351 (1958).
[63] Granier, J. and Astoin, N., Compt. Rend. 242, 1431-1433 (1956).
[64] Astoin, N. and Granier, J., Compt. Rend. 241, 1736-1738 (1955).

[65] Nakayama, T., Kitamura, Y. and Watanabe, K., J. Chem. Phys. 30, 5, 1180-1186 (1959).
[66] Watanabe, K., J. Chem. Phys. 26, 3, 542-547 (1957).
[67] Astoin, N., Compt. Rend. 242, 2327-2329 (1956).
[68] Sun, H. and Weissler, G. L., J. Chem. Phys. 23, 6, 1160-1165 (1955).
[69] Ditchburn, R. W., Proc. Roy. Soc. (London) A229, 44-62 (1955).

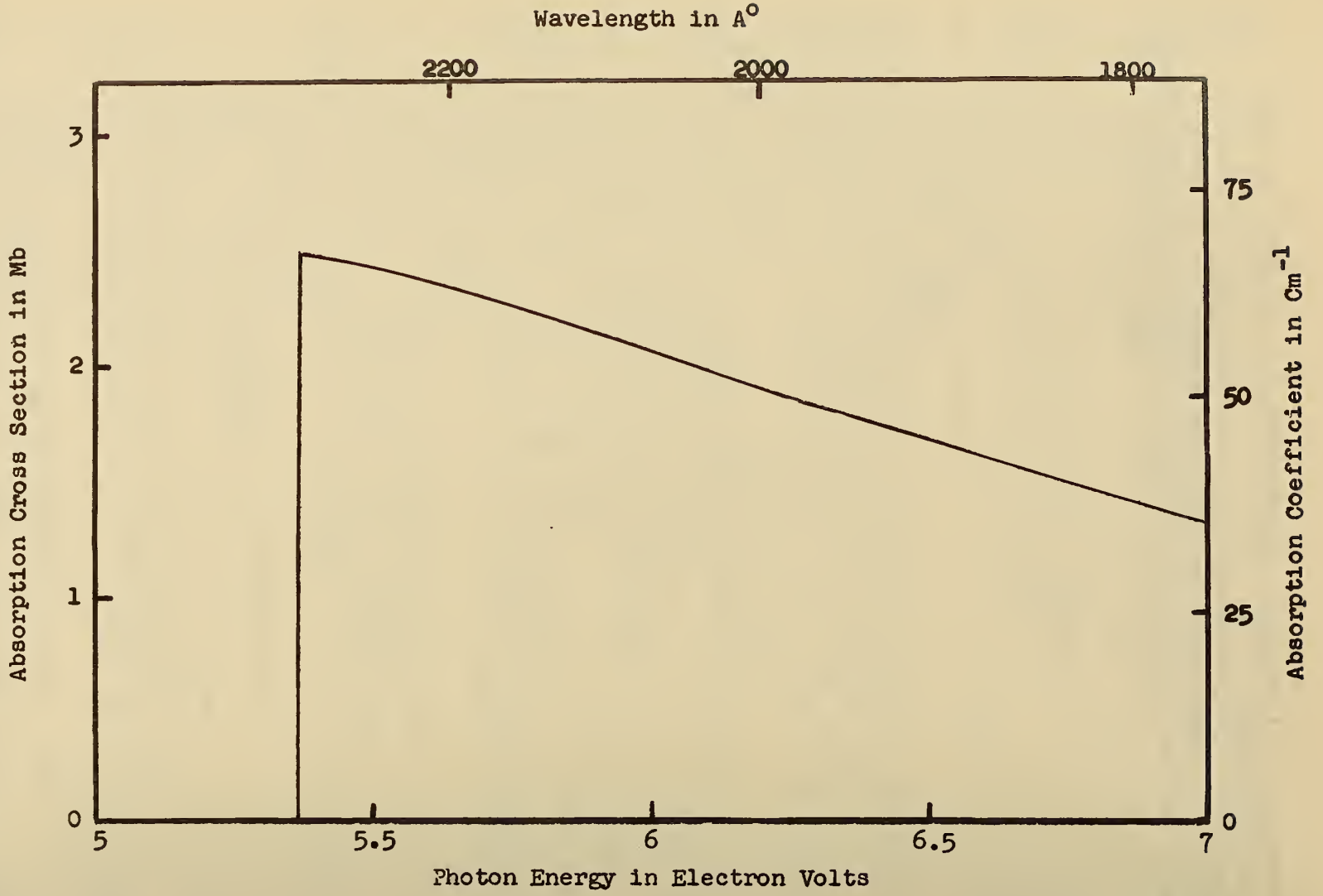

Figure 1. The atomic absorption cross section of lithium [15,17].

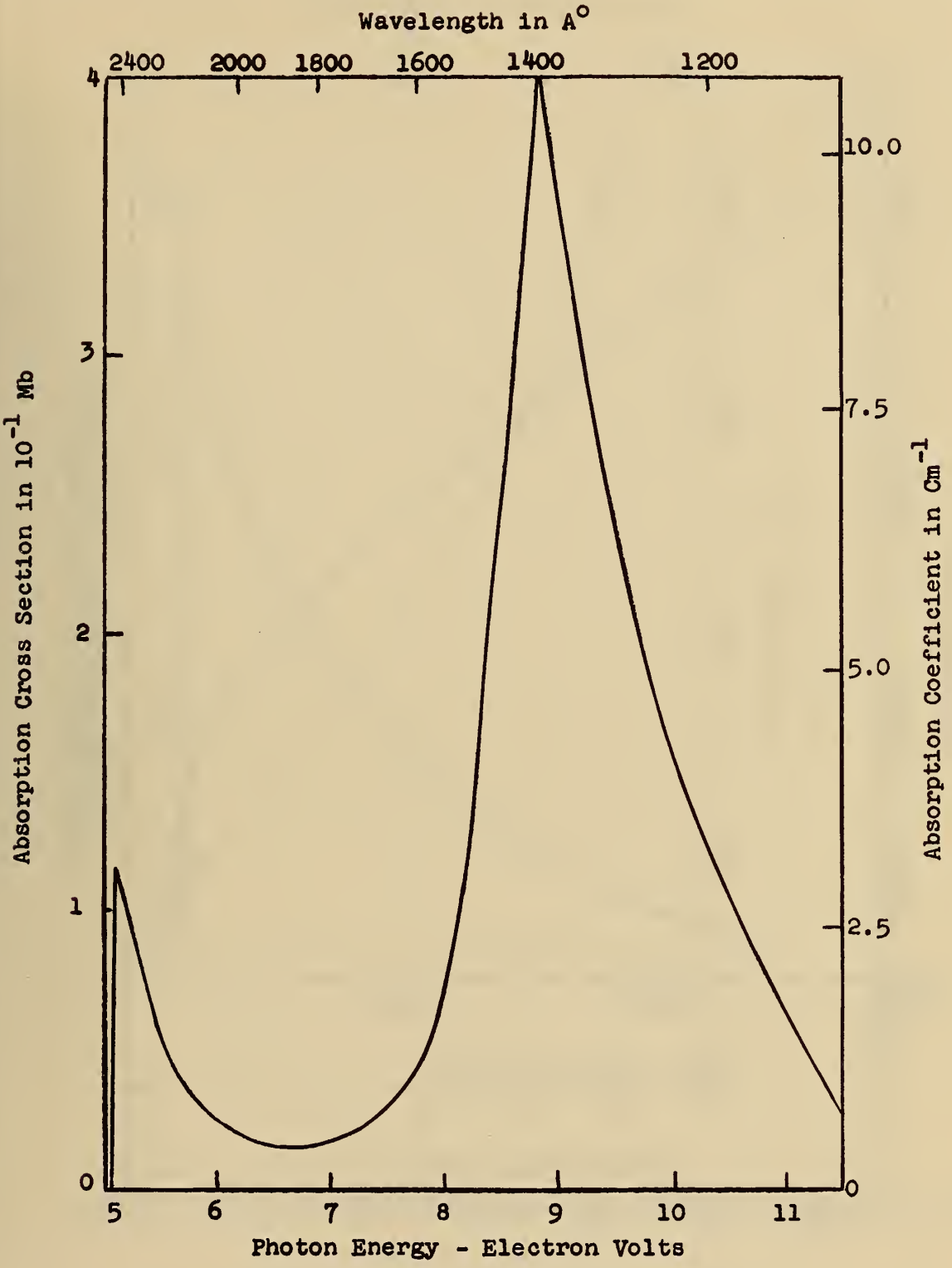

Figure 2. The atomic absorption cross section of sodium [17,18].

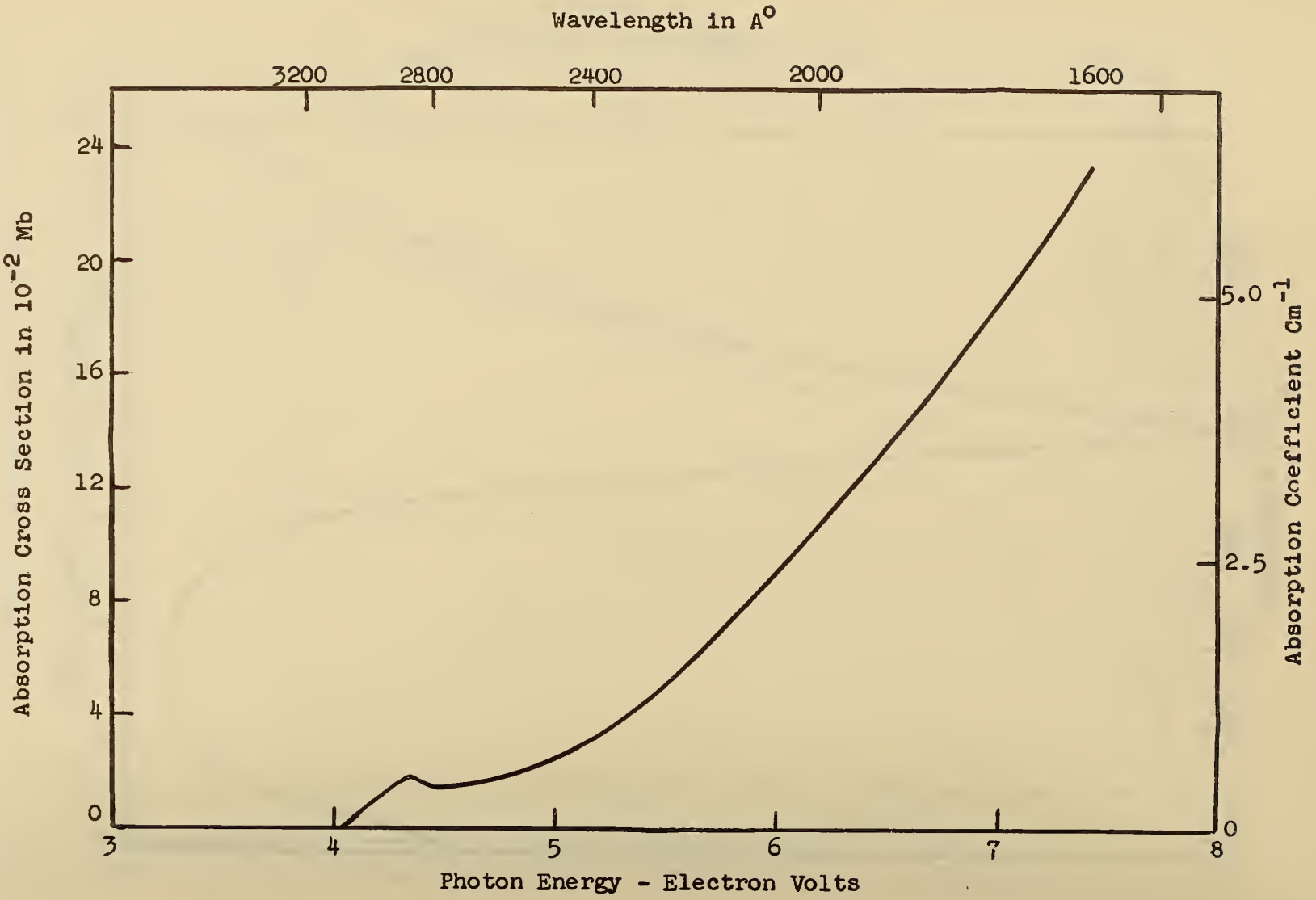

Figure 3. The atomic absorption cross section of potassium [18].

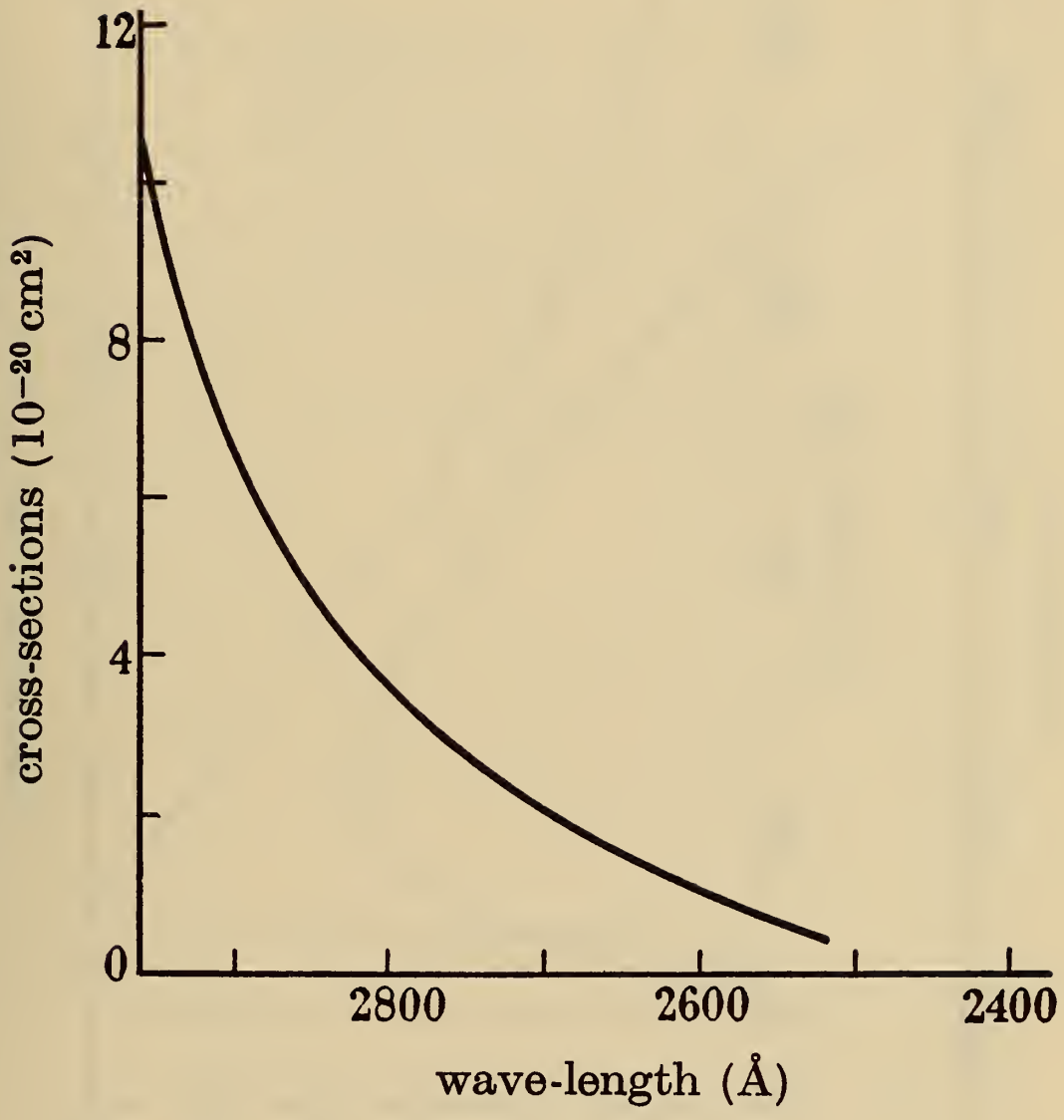

Figure 4. The atomic photoionization cross section of rubidium [19].

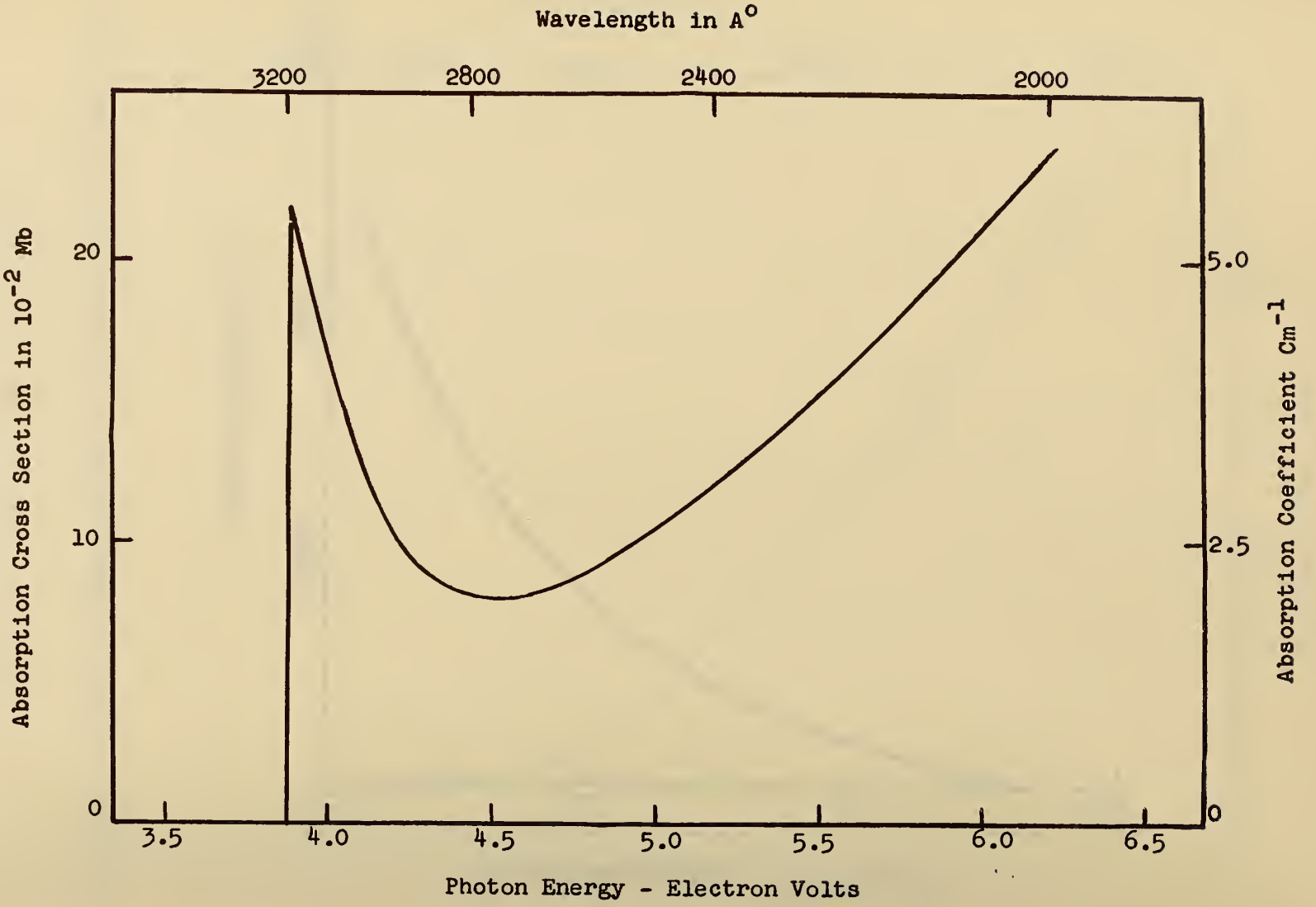

Figure 5. The atomic absorption cross section of cesium [22].

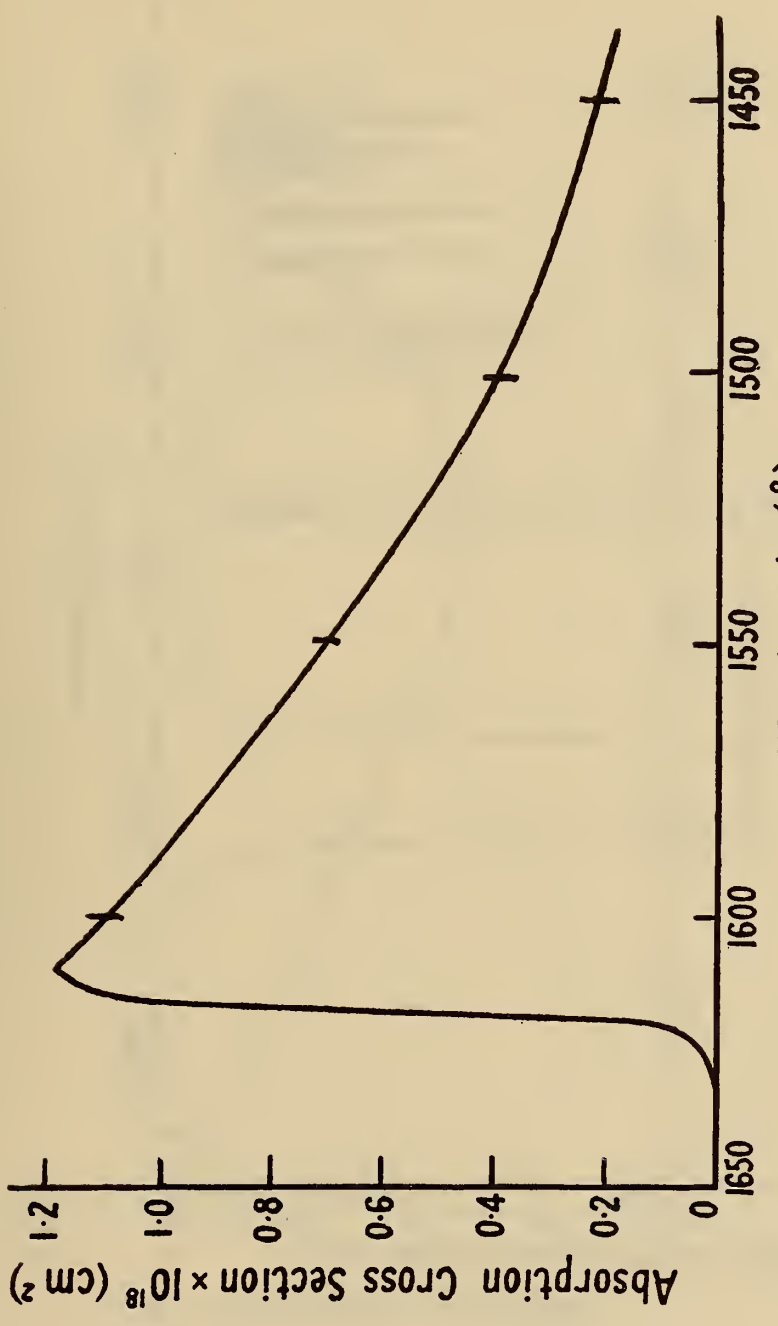

Figure 6. The atomic absorption cross section of magnesium [24].

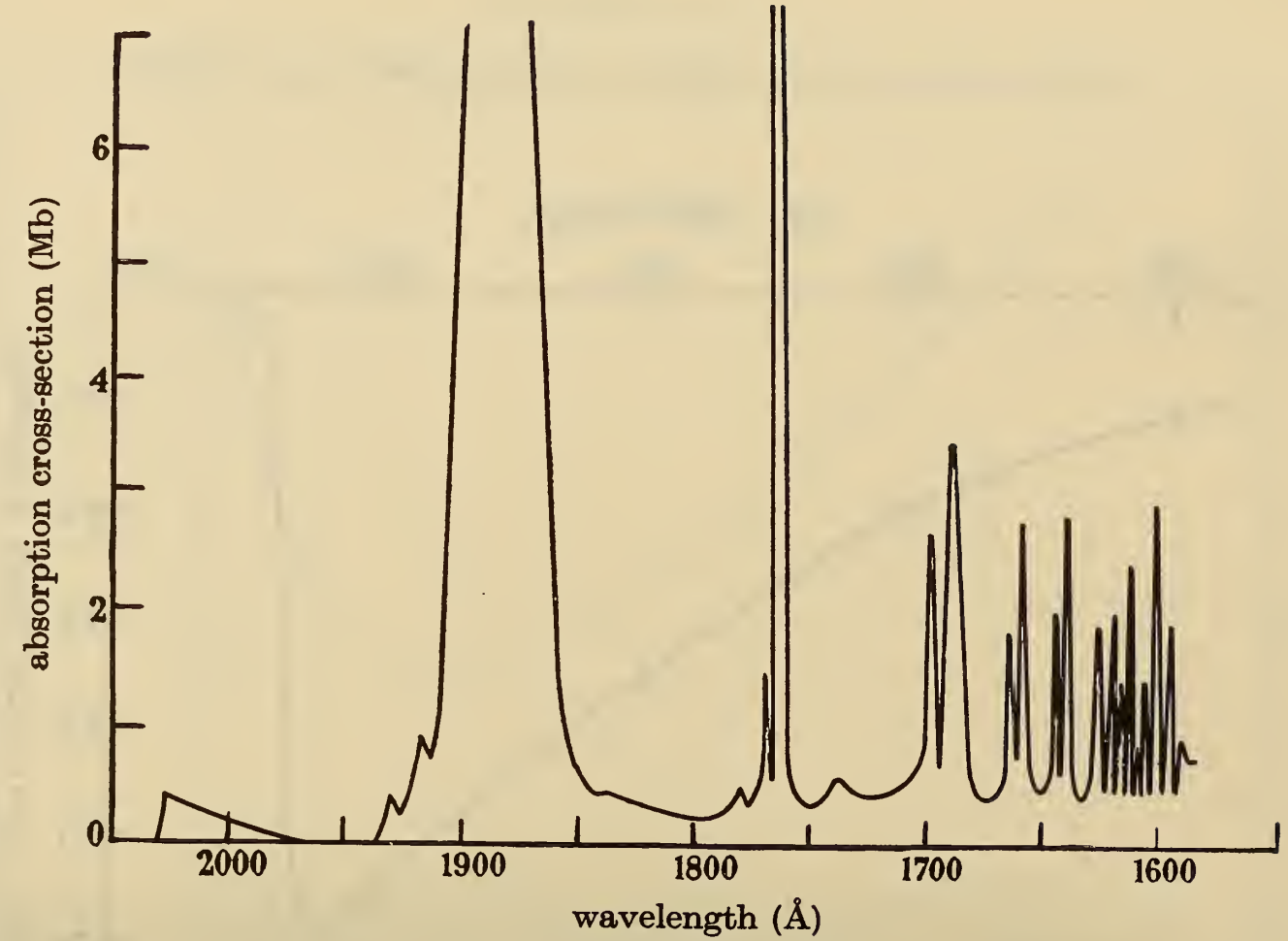

Figure 7. The atomic absorption cross section of calcium from 2028A to 1600A showing autoionization by line absorption superposed on a small continuum [25].

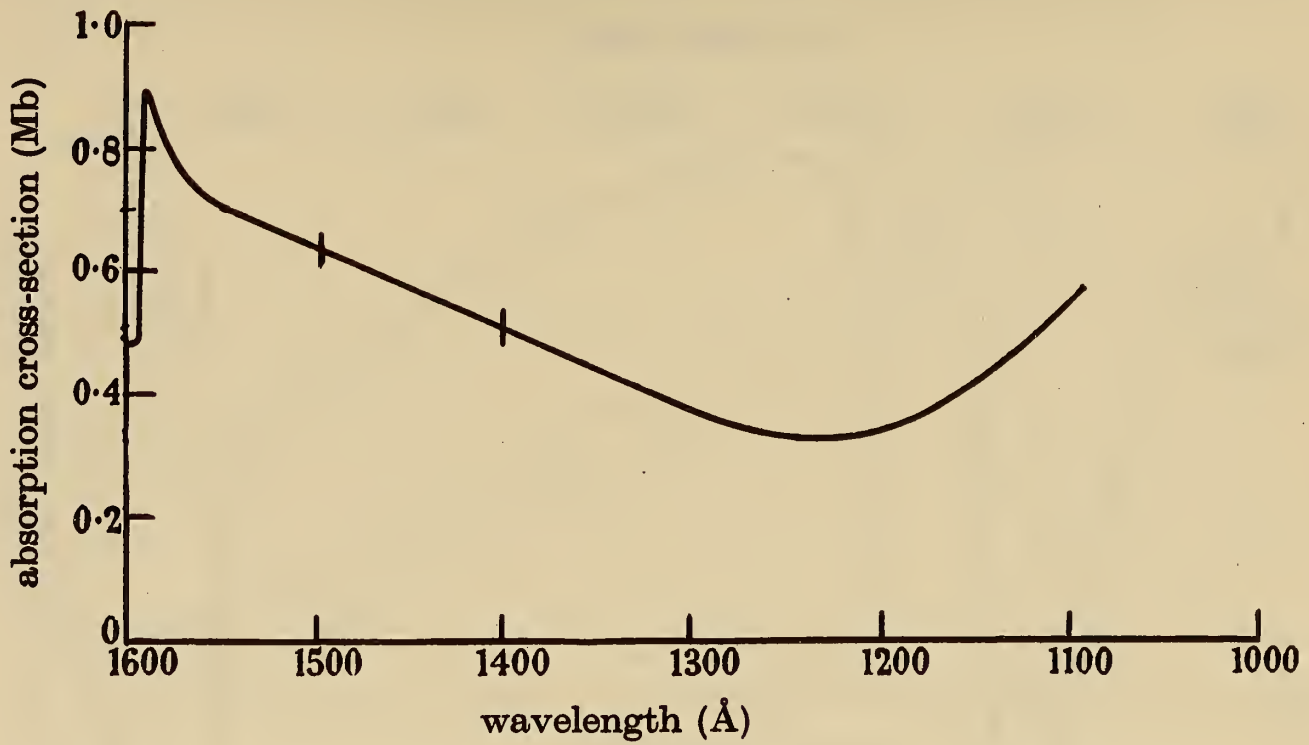

Figure 8. The atomic absorption cross section of calcium from 1600A to 1080A [25].

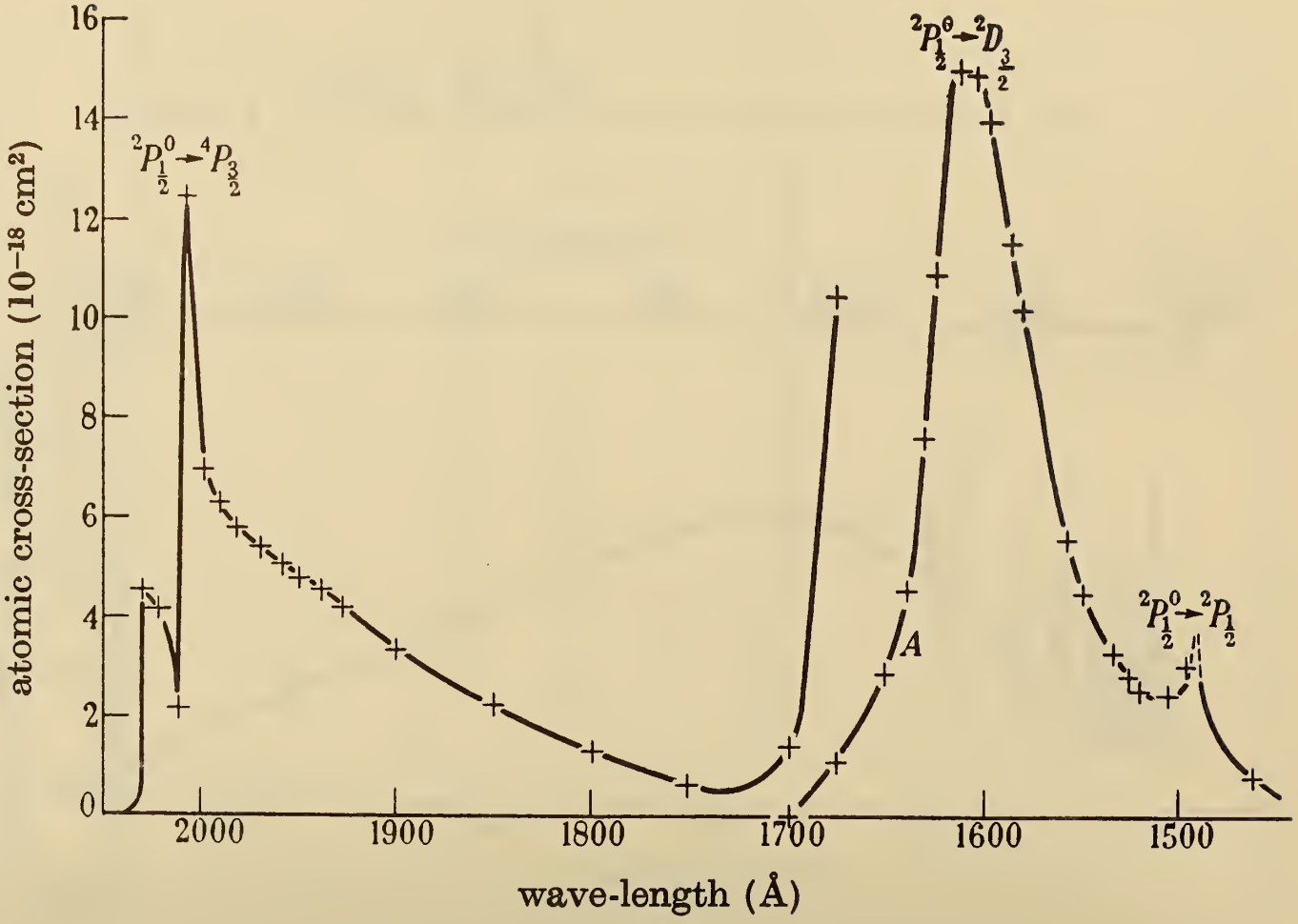

Figure 9. The atomic absorption cross section of thallium. In curve A from 1700A to 1450A the ordinate scale is 10^{-17} cm^2. Three peaks from line absorption giving autoionization are indicated [27].

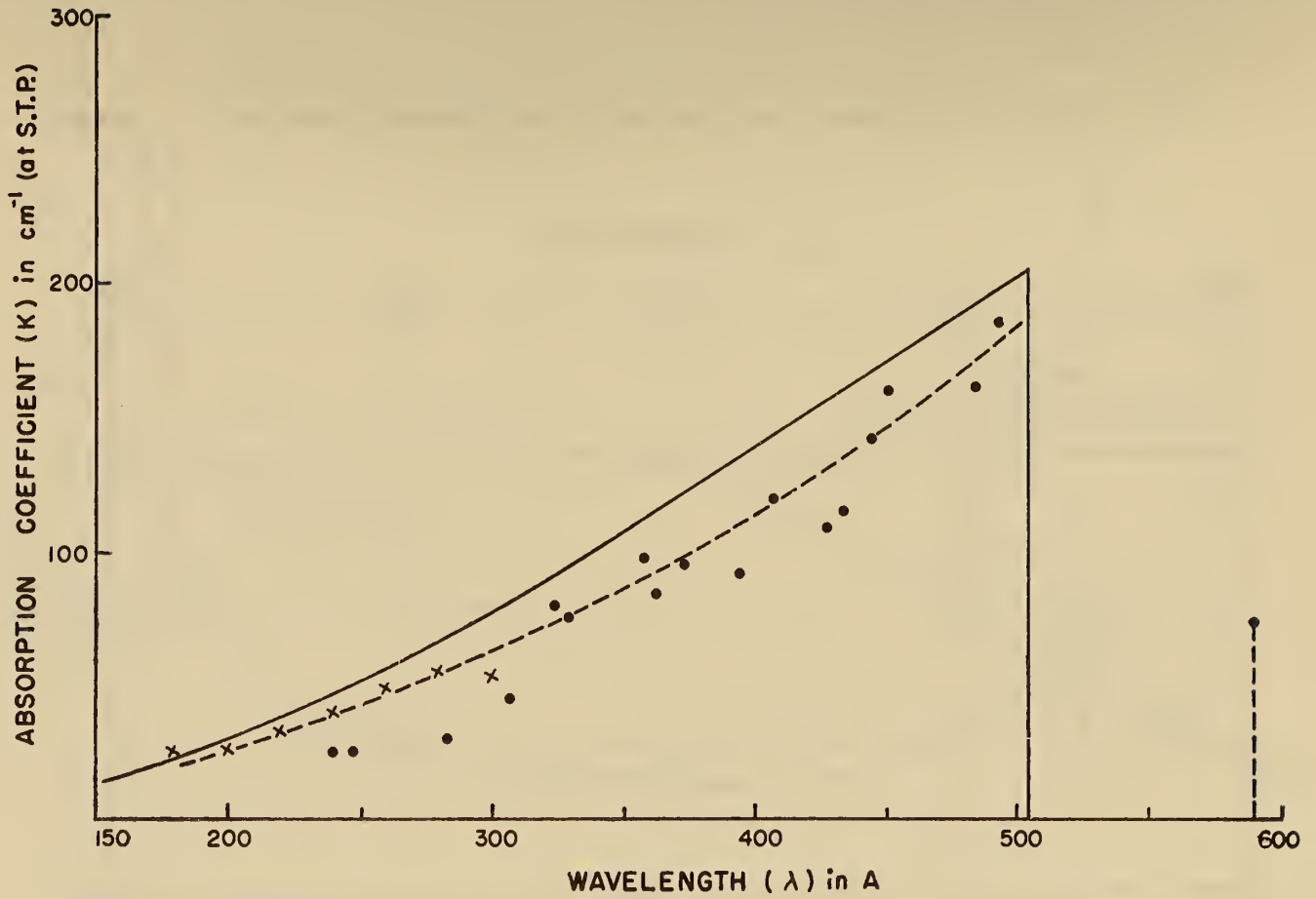

Figure 10. The absorption coefficient of helium. ($\sigma = 3.7 \times 10^{-20}$ K) Solid line theoretical curve, dashed curve and crosses from Axelrod and Givens [32] and dots from Lee and Weissler [31].

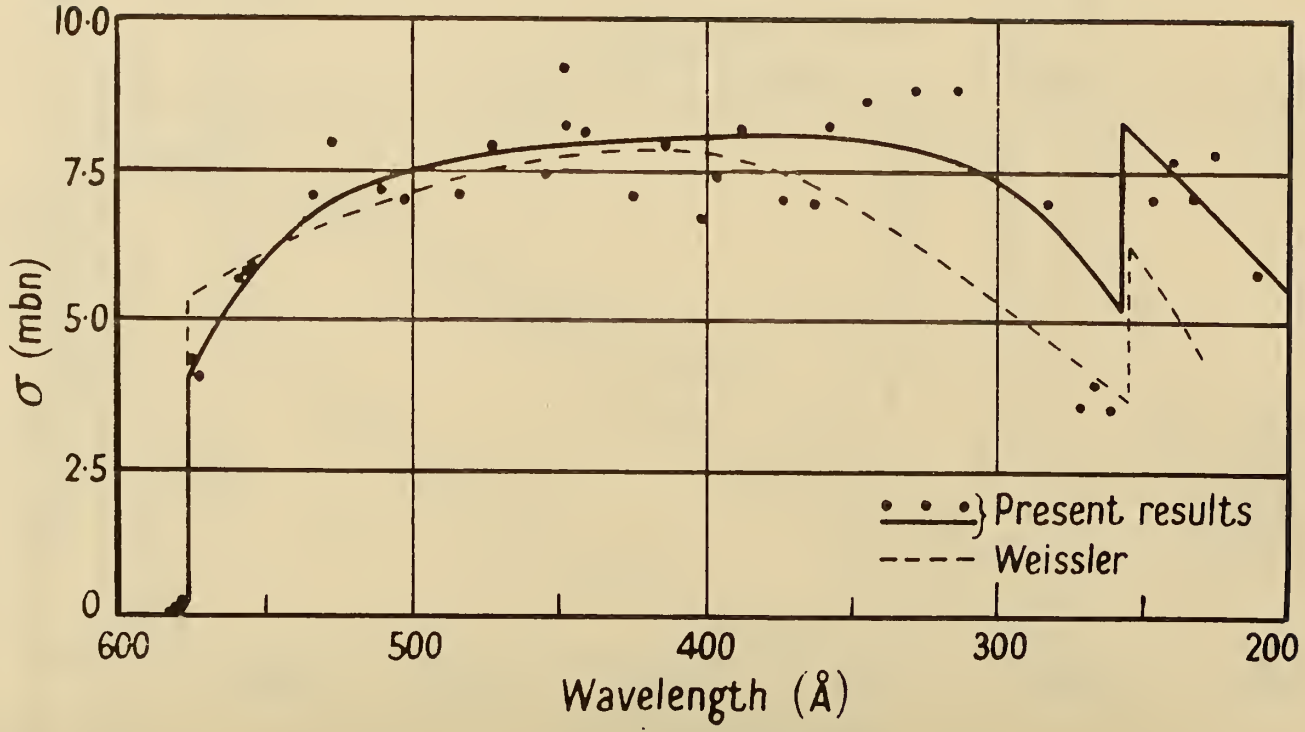

Figure 11. The atomic absorption cross section of neon from Ditchburn [36].

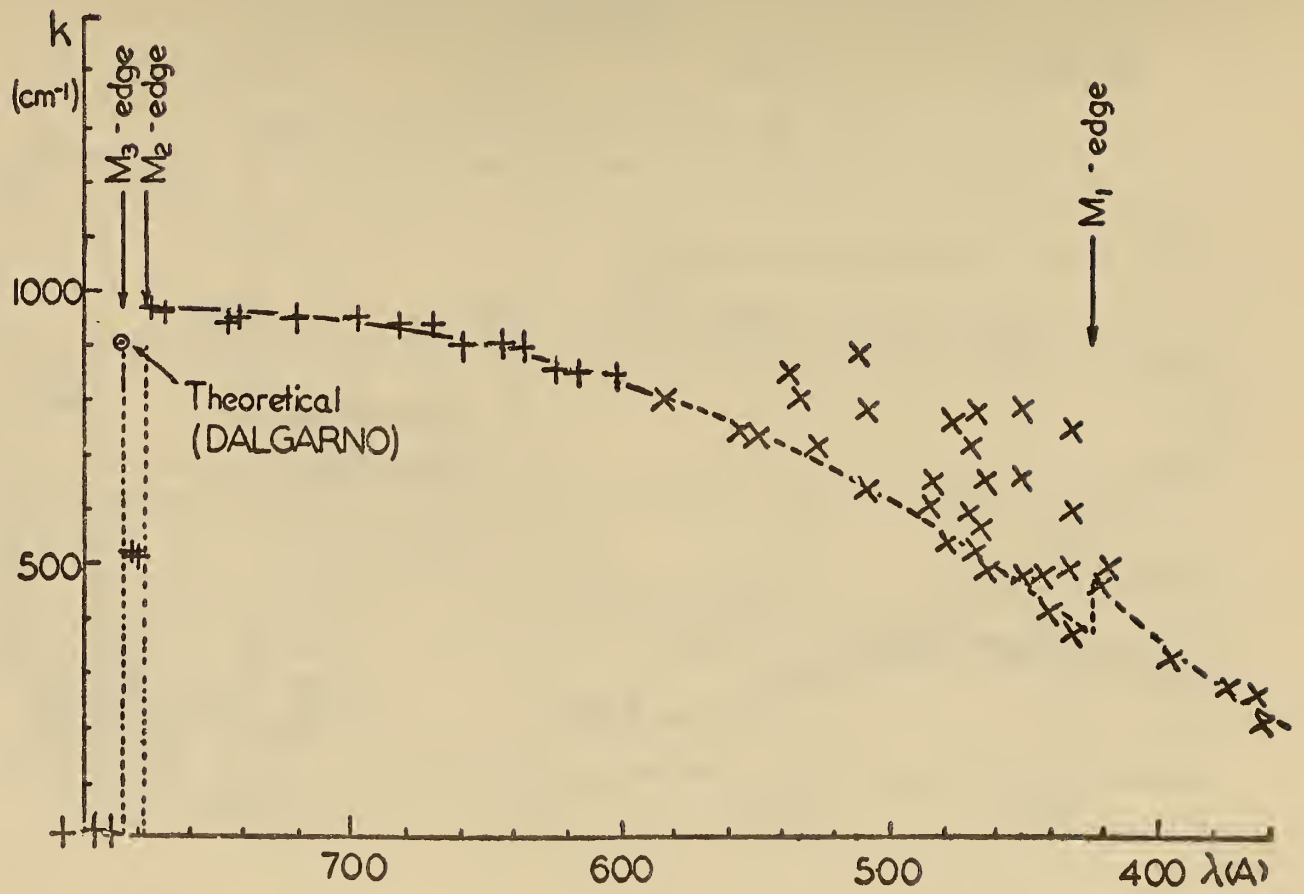

Figure 12. The absorption coefficient of argon from Lee and Weissler [35].

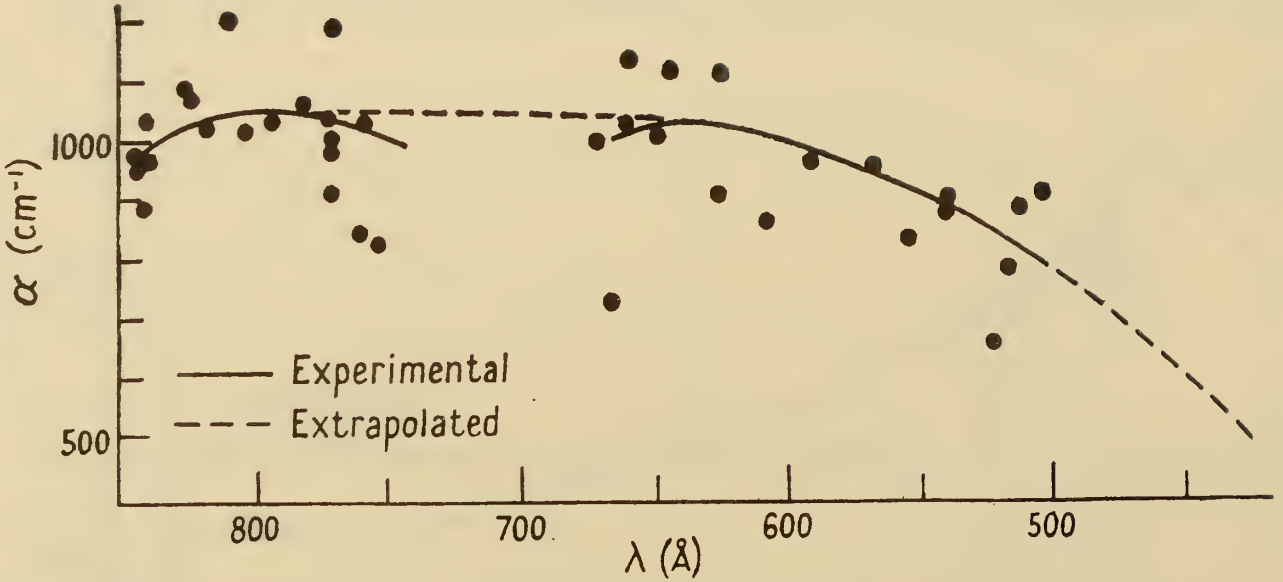

Figure 13. The absorption coefficient for continuous absorption in krypton from Pery-Thorne and Garton [39].

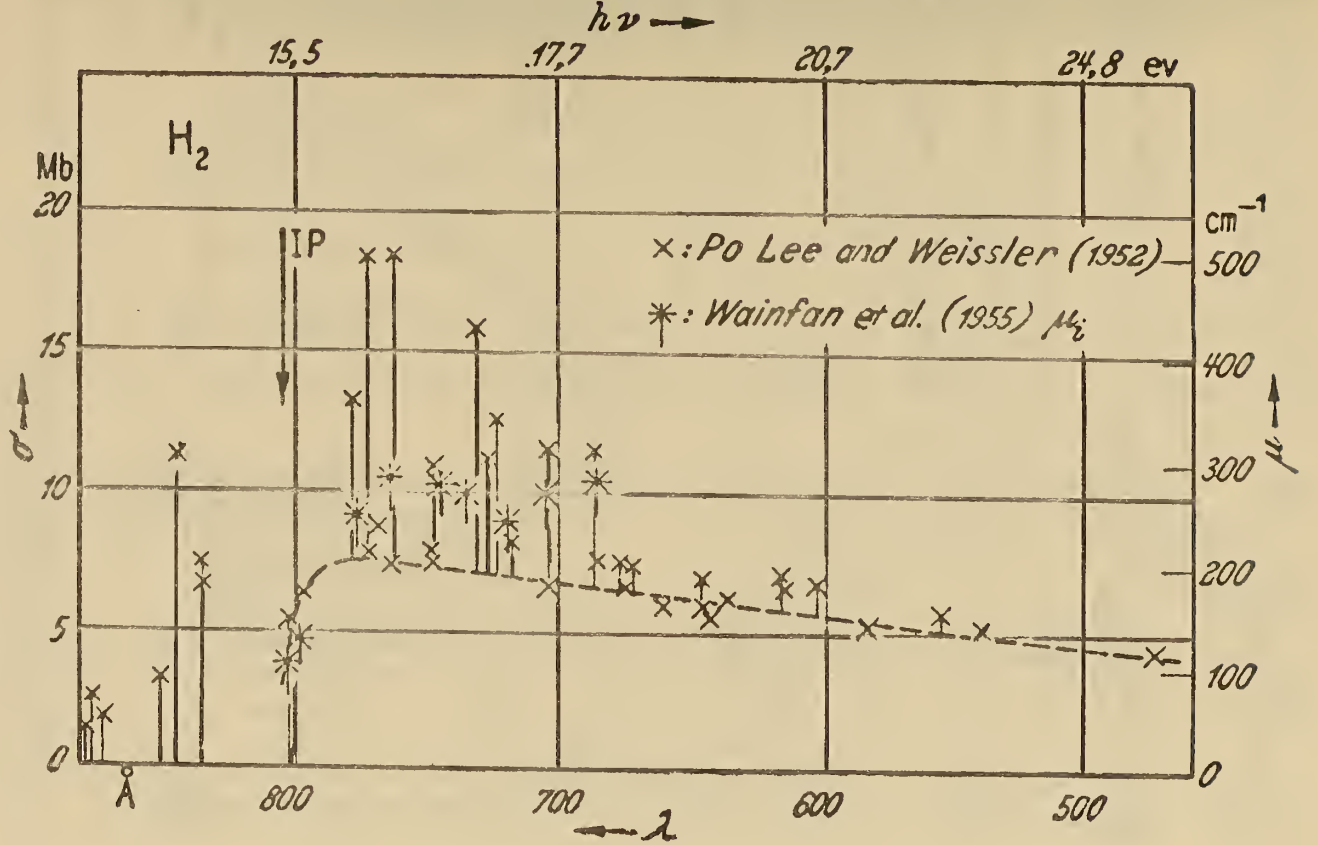

Figure 14. The molecular cross section for absorption and ionization in hydrogen [41,38,1].

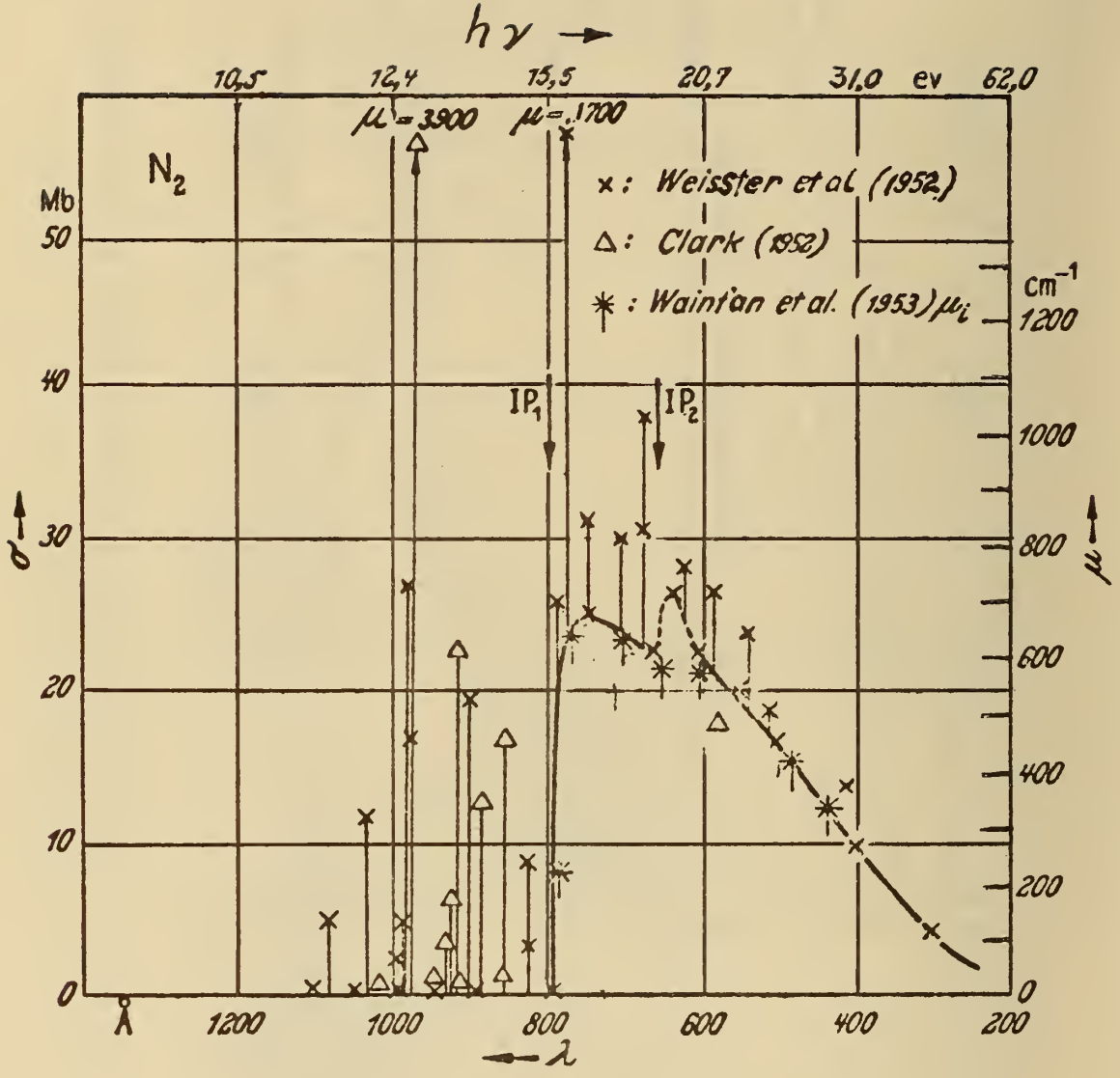

Figure 15. The molecular cross section for absorption and ionization in nitrogen [44,38,1].

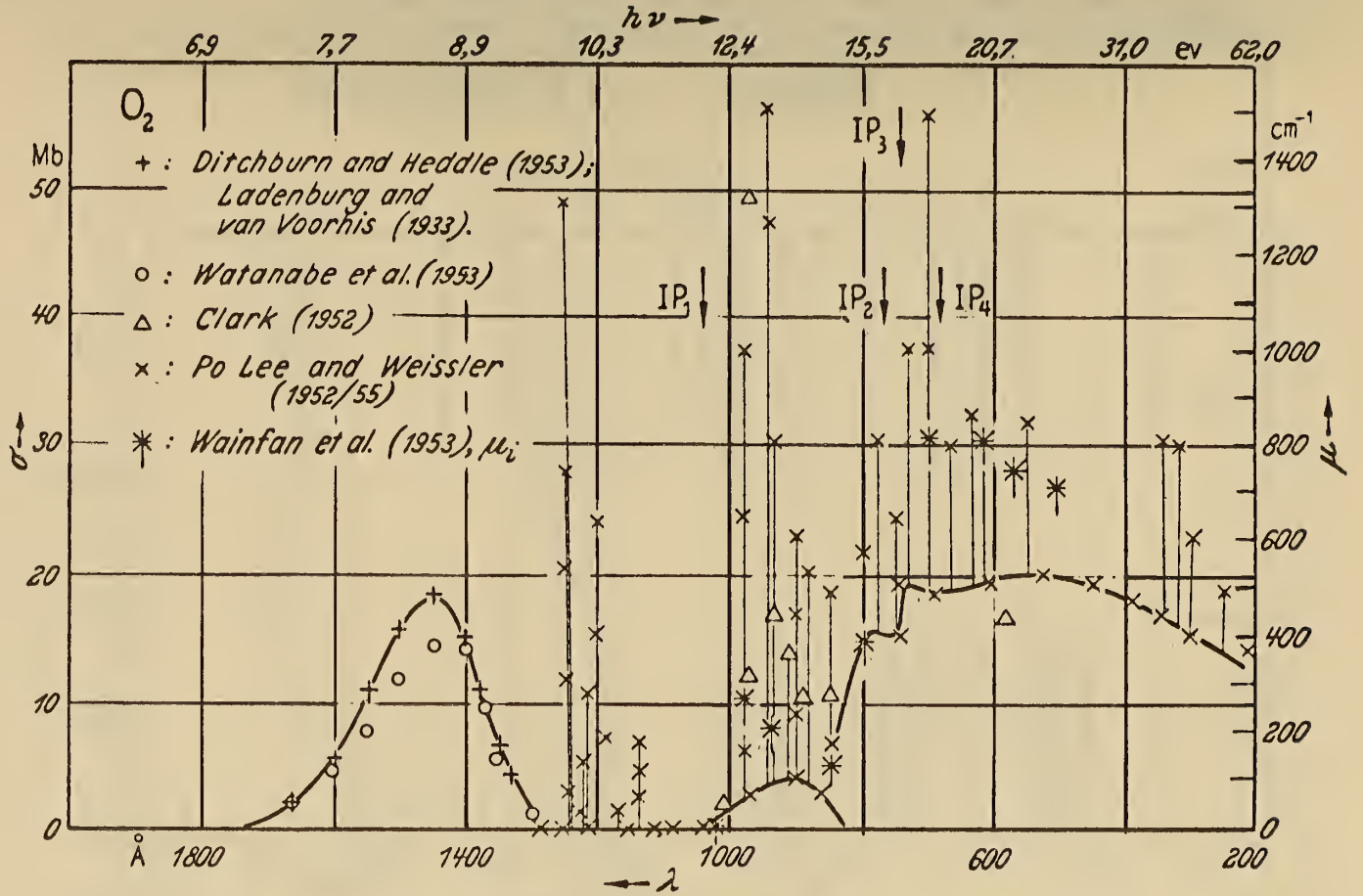

Figure 16. The molecular cross section for absorption and ionization in oxygen [50,38,i].

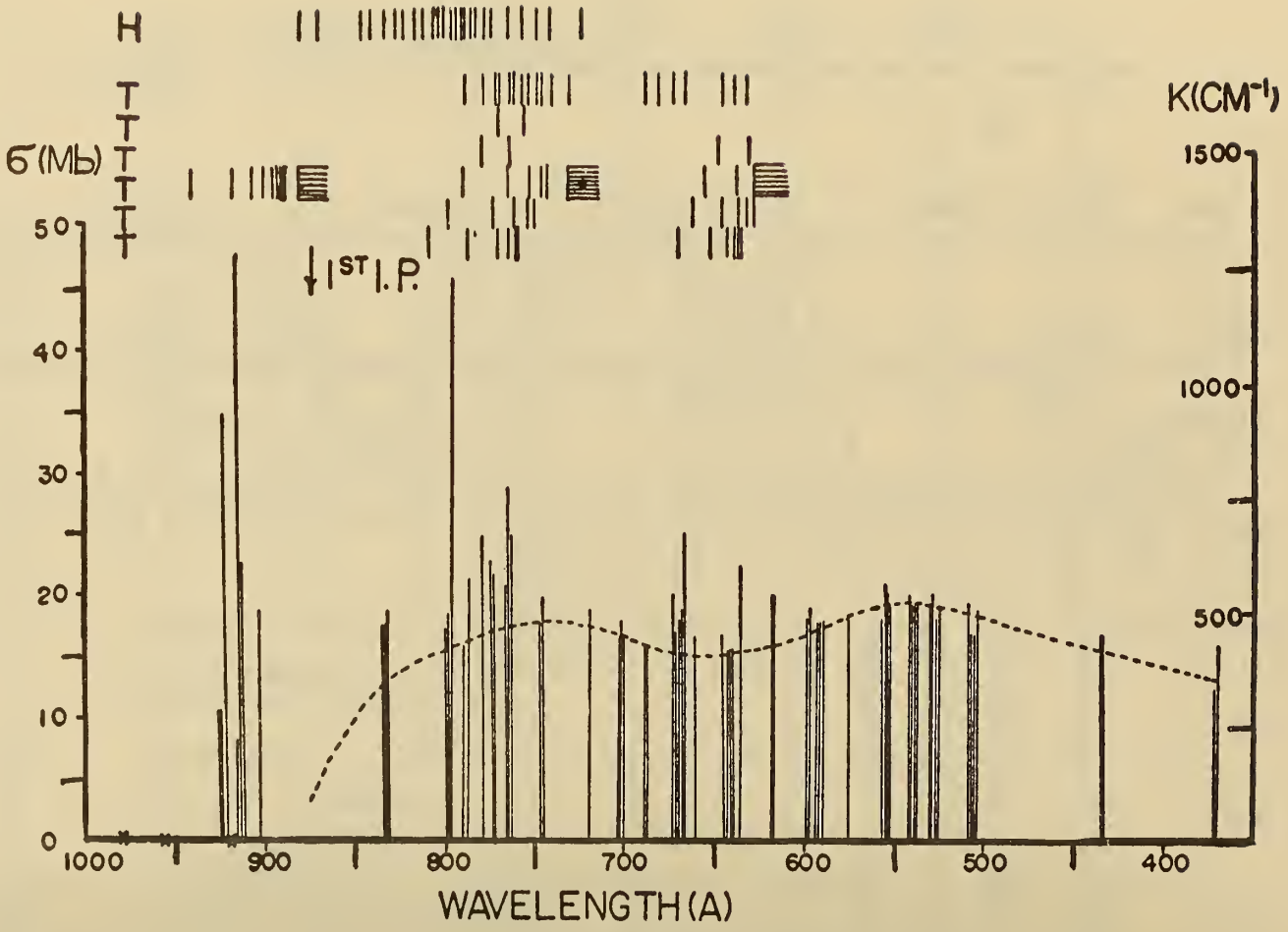

Figure 17. The molecular absorption cross section of carbon monoxide. Dotted curve is continuum [55]. Short lines in upper left show band systems.

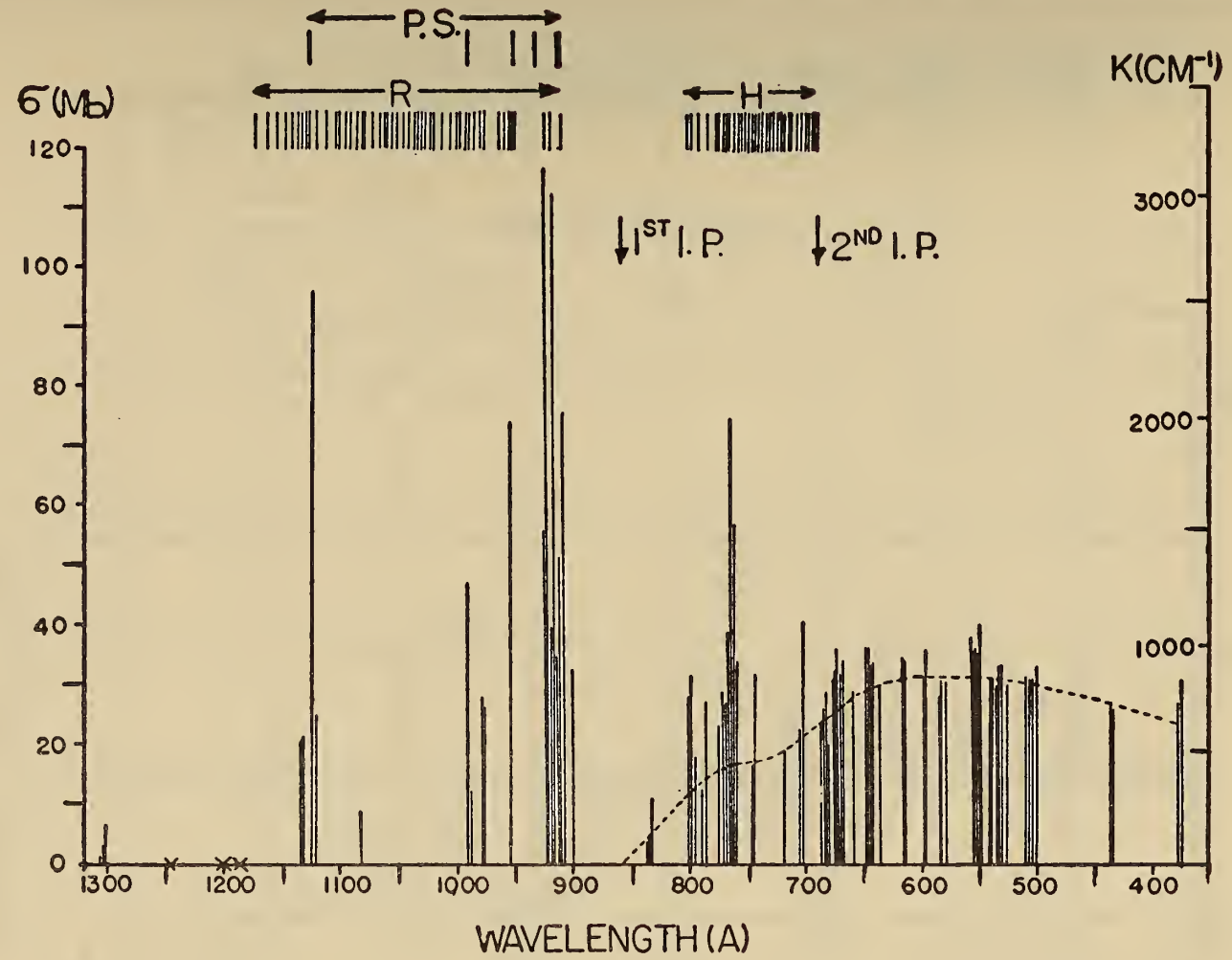

Figure 18. Molecular absorption cross section of carbon dioxide. Dotted curve is ionization continuum [55]. Above shows two band systems.

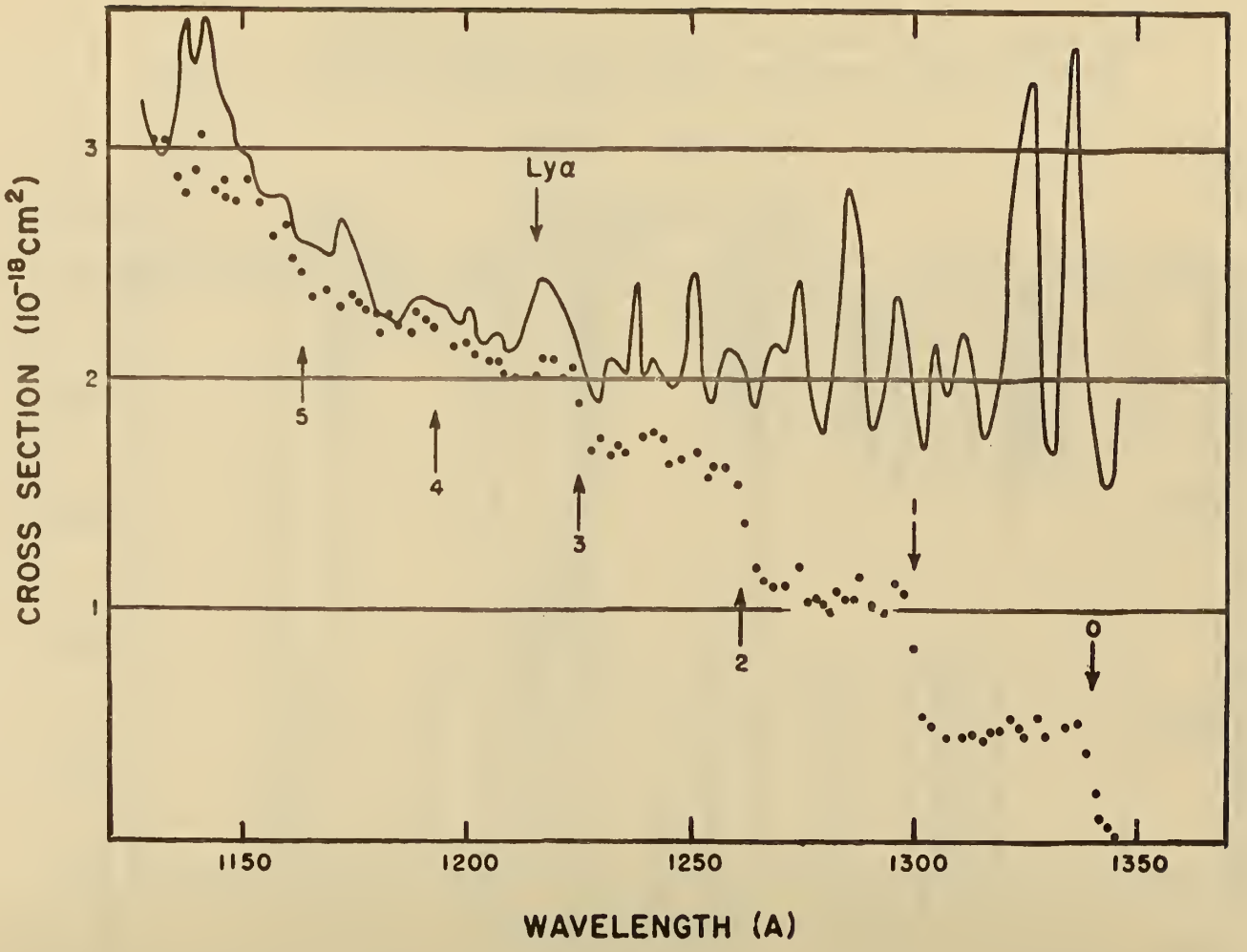

Figure 19. Molecular cross sections for absorption (solid curve) and ionization (dots) in nitric oxide [59]. Arrows show vibration structure.

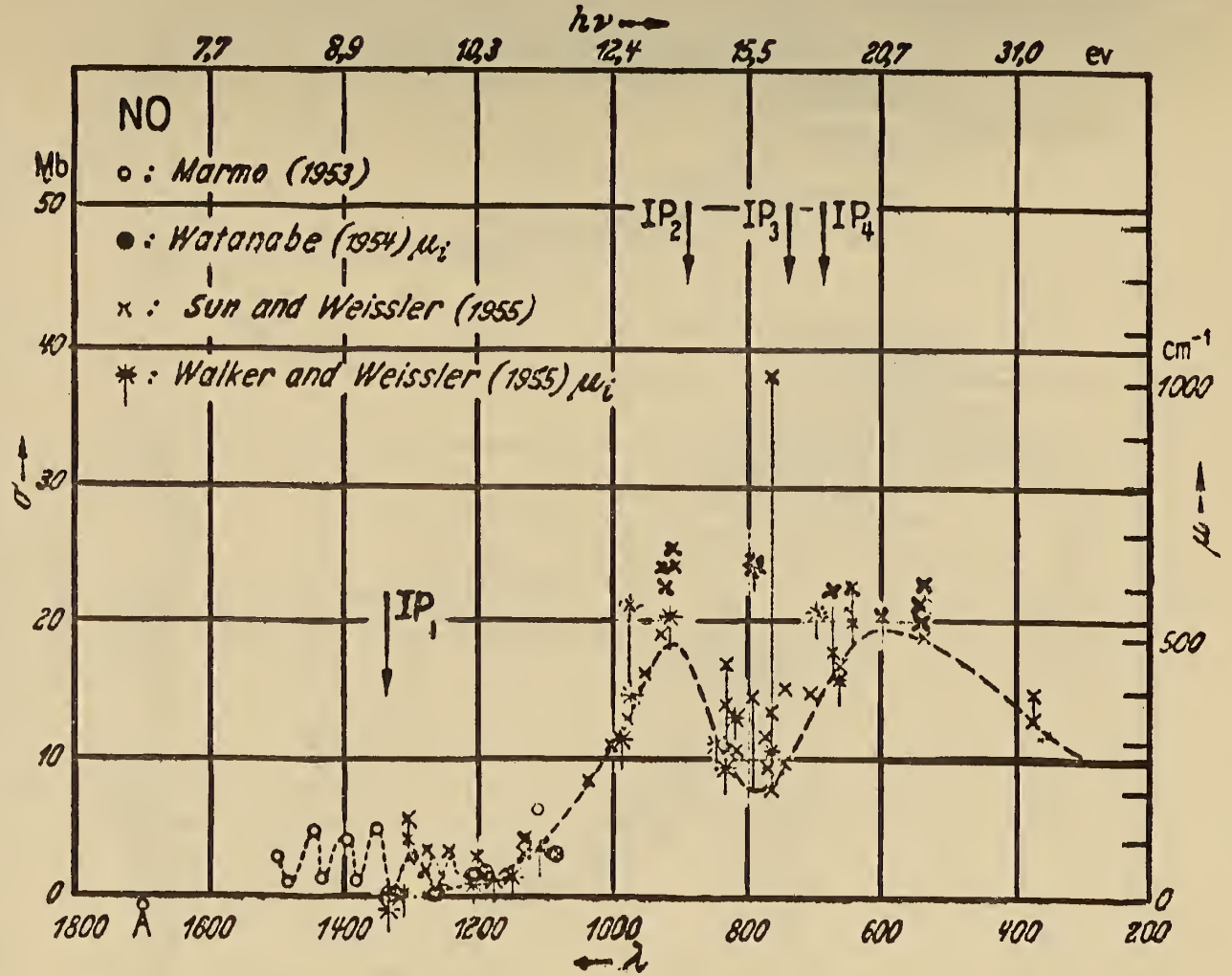

Figure 20. Molecular cross sections for absorption and ionization of NO in far ultraviolet [1].

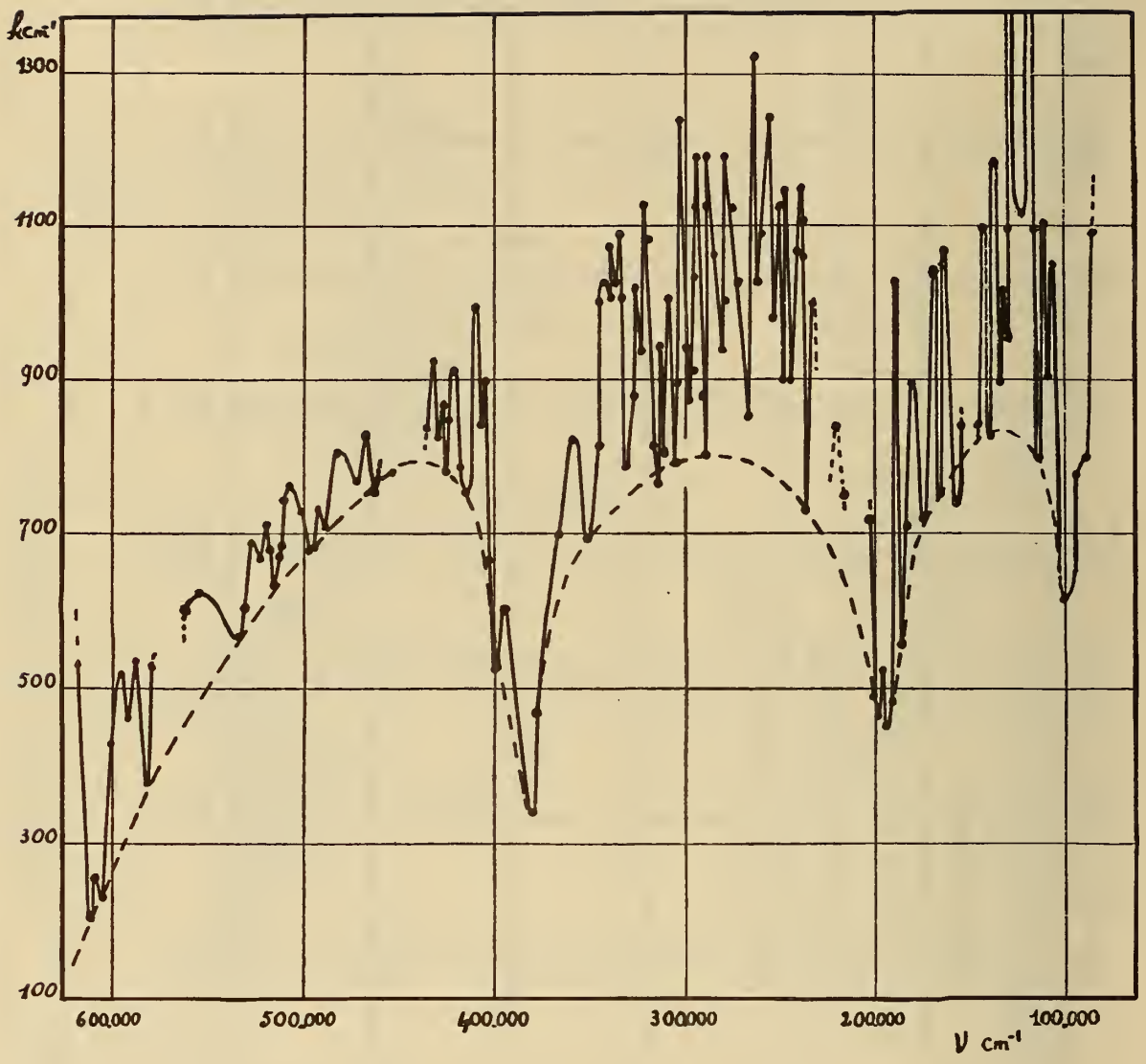

Figure 21. Molecular absorption coefficient of nitrous oxide as a function of wave number. Dashed curve is continuous absorption. (Astoin and Granier [64].)

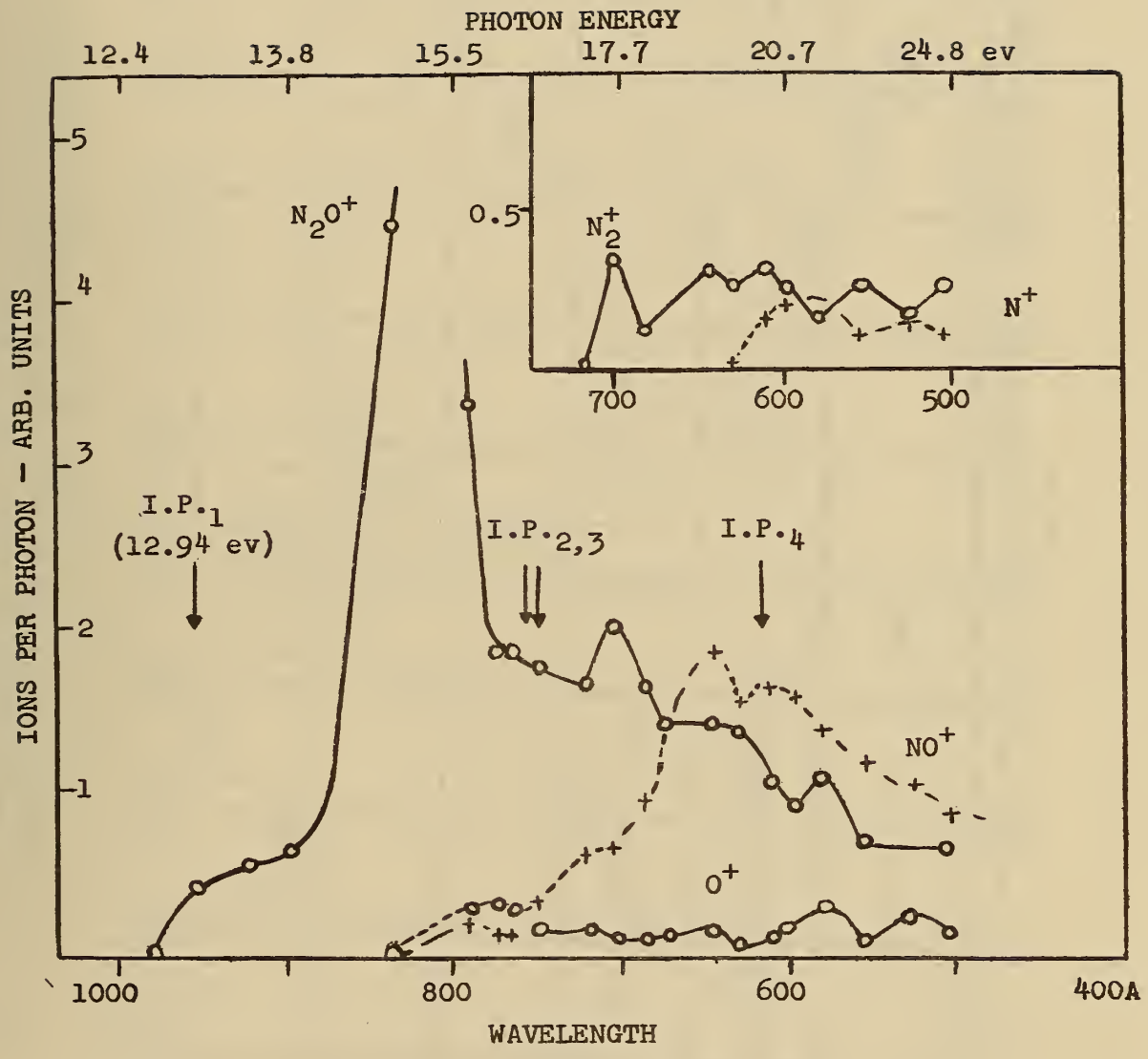

Figure 22. Ions produced by photoionization of nitrous oxide in a mass spectrometer [46].

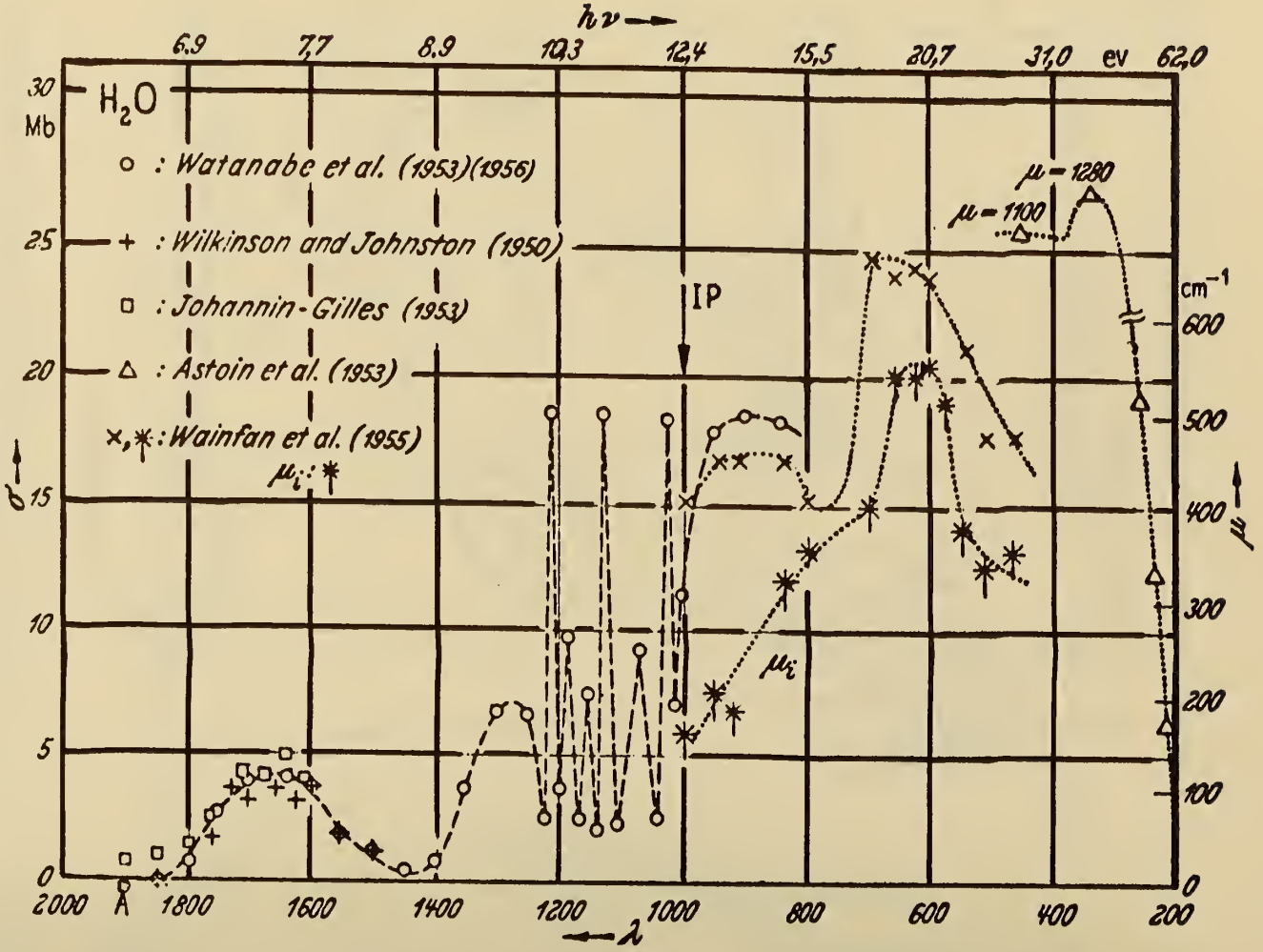

Figure 23. Molecular cross sections for absorption and photoionization of water vapor [1].

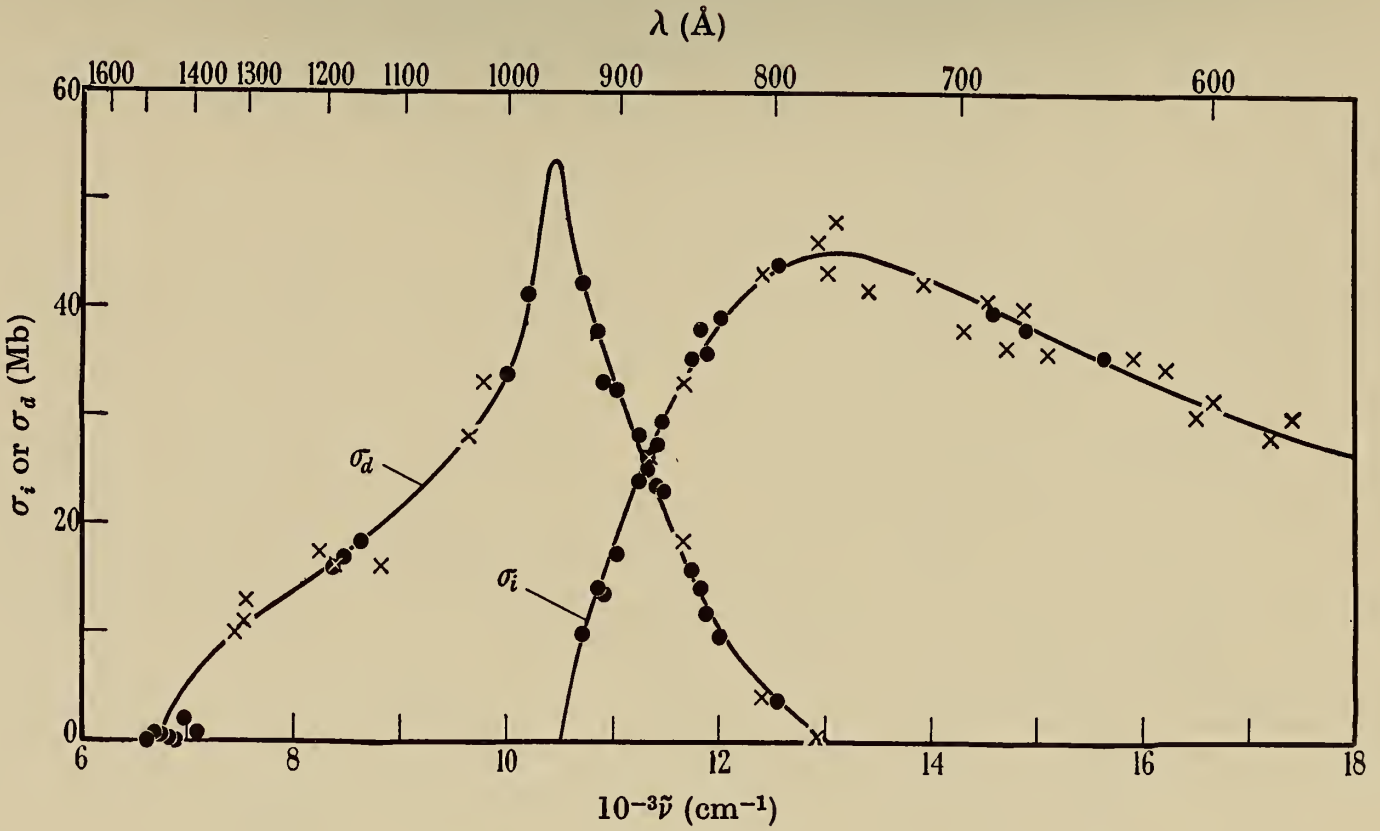

Figure 24. Molecular cross section for absorption and photoionization of methane. (Ditchburn [69] using data of Wainfan, et al., [38] on photoionization efficiency.)

U. S. DEPARTMENT OF COMMERCE
Luther H. Hodges, *Secretary*

NATIONAL BUREAU OF STANDARDS
A. V. Astin, *Director*

THE NATIONAL BUREAU OF STANDARDS

The scope of activities of the National Bureau of Standards at its major laboratories in Washington, D.C., and Boulder, Colorado, is suggested in the following listing of the divisions and sections engaged in technical work. In general, each section carries out specialized research, development, and engineering in the field indicated by its title. A brief description of the activities, and of the resultant publications, appears on the inside of the front cover.

WASHINGTON, D.C.

Electricity. Resistance and Reactance. Electrochemistry. Electrical Instruments. Magnetic Measurements. Dielectrics. High Voltage.

Metrology. Photometry and Colorimetry. Refractometry. Photographic Research. Length. Engineering Metrology. Mass and Scale. Volumetry and Densimetry.

Heat. Temperature Physics. Heat Measurements. Cryogenic Physics. Equation of State. Statistical Physics.

Radiation Physics. X-ray. Radioactivity. Radiation Theory. High Energy Radiation. Radiological Equipment. Nucleonic Instrumentation. Neutron Physics.

Analytical and Inorganic Chemistry. Pure Substances. Spectrochemistry. Solution Chemistry. Standard Reference Materials. Applied Analytical Research.

Mechanics. Sound. Pressure and Vacuum. Fluid Mechanics. Engineering Mechanics. Rheology. Combustion Controls.

Organic and Fibrous Materials. Rubber. Textiles. Paper. Leather. Testing and Specifications. Polymer Structure. Plastics. Dental Research.

Metallurgy. Thermal Metallurgy. Chemical Metallurgy. Mechanical Metallurgy. Corrosion. Metal Physics. Electrolysis and Metal Deposition.

Mineral Products. Engineering Ceramics. Glass. Refractories. Enameled Metals. Crystal Growth. Physical Properties. Constitution and Microstructure.

Building Research. Structural Engineering. Fire Research. Mechanical Systems. Organic Building Materials. Codes and Safety Standards. Heat Transfer. Inorganic Building Materials.

Applied Mathematics. Numerical Analysis. Computation. Statistical Engineering. Mathematical Physics. Operations Research.

Data Processing Systems. Components and Techniques. Computer Technology. Measurements Automation. Engineering Applications. Systems Analysis.

Atomic Physics. Spectroscopy. Infrared Spectroscopy. Solid State Physics. Electron Physics. Atomic Physics.

Instrumentation. Engineering Electronics. Electron Devices. Electronic Instrumentation. Mechanical Instruments. Basic Instrumentation.

Physical Chemistry. Thermochemistry. Surface Chemistry. Organic Chemistry. Molecular Spectroscopy. Molecular Kinetics. Mass Spectrometry.

Office of Weights and Measures.

BOULDER, COLO.

Cryogenic Engineering. Cryogenic Equipment. Cryogenic Processes. Properties of Materials. Cryogenic Technical Services.

Ionosphere Research and Propagation. Low Frequency and Very Low Frequency Research. Ionosphere Research. Prediction Services. Sun-Earth Relationships. Field Engineering. Radio Warning Services. Vertical Soundings Research.

Radio Propagation Engineering. Data Reduction Instrumentation. Radio Noise. Tropospheric Measurements. Tropospheric Analysis. Propagation-Terrain Effects. Radio-Meteorology. Lower Atmosphere Physics.

Radio Standards. High Frequency Electrical Standards. Radio Broadcast Service. Radio and Microwave Materials. Atomic Frequency and Time Interval Standards. Electronic Calibration Center. Millimeter-Wave Research. Microwave Circuit Standards.

Radio Systems. Applied Electromagnetic Theory. High Frequency and Very High Frequency Research. Modulation Research. Antenna Research. Navigation Systems.

Upper Atmosphere and Space Physics. Upper Atmosphere and Plasma Physics. Ionosphere and Exosphere Scatter. Airglow and Aurora. Ionospheric Radio Astronomy.


NBS